T.R.

GEBZE TECHNICAL UNIVERSITY

GRADUATE SCHOOL OF NATURAL AND APPLIED SCIENCES

INVESTIGATION OF ELECTRICAL PROPERTIES OF $Pb(Ni_{1/3}Nb_{2/3})O_3$-$Pb(Zr,Ti)O_3$ (PNN-PZT) CERAMICS AND THEIR DEVICE APPLICATIONS

MEHMET GÜRKAN ÖZYAZICI

A THESIS SUBMITTED FOR THE DEGREE OF

MASTER OF SCIENCE

DEPARTMENT OF MATERIALS SCIENCE AND ENGINEERING

GEBZE

2018

T.R.

GEBZE TECHNICAL UNIVERSITY

GRADUATE SCHOOL OF NATURAL AND APPLIED SCIENCES

INVESTIGATION OF ELECTRICAL PROPERTIES OF $Pb(Ni_{1/3}Nb_{2/3})O_3$-$Pb(Zr,Ti)O_3$ (PNN-PZT) CERAMICS AND THEIR DEVICE APPLICATIONS

MEHMET GÜRKAN ÖZYAZICI

A THESIS SUBMITTED FOR THE DEGREE OF MASTER OF SCIENCE

DEPARTMENT OF MATERIALS SCIENCE AND ENGINEERING

THESIS SUPERVISOR

ASSOC. PROF. DR. EBRU MENŞUR ALKOY

GEBZE

2018

GEBZE TEKNİK ÜNİVERSİTESİ	YÜKSEK LİSANS JÜRİ ONAY FORMU

GTÜ Fen Bilimleri Enstitüsü Yönetim Kurulu'nun 17/01/2018 tarih ve 2018/04 sayılı kararıyla oluşturulan jüri tarafından 09/02/2018 tarihinde tez savunma sınavı yapılan Mehmet Gürkan ÖZYAZICI'ın tez çalışması Malzeme Bilimi ve Mühendisliği Anabilim Dalında YÜKSEK LİSANS tezi olarak kabul edilmiştir.

JÜRİ

ÜYE (TEZ DANIŞMANI)	:Doç. Dr. Ebru MENŞUR ALKOY
ÜYE	:Yrd. Doç. Dr. Aligül BÜYÜKAKSOY
ÜYE	:Yrd. Doç. Dr. Ali AKMAN

ONAY

Gebze Teknik Üniversitesi Fen Bilimleri Enstitüsü Yönetim Kurulu'nun

...../...../..... tarih ve ...../..... sayılı kararı.

T.C.
GEBZE TEKNİK ÜNİVERSİTESİ
FEN BİLİMLERİ ENSTİTÜSÜ

$Pb(Ni_{1/3}Nb_{2/3})O_3$-$Pb(Zr,Ti)O_3$ (PNN-PZT) SERAMİKLERİN ELEKTRİKSEL ÖZELLİKLERİNİN VE CİHAZ UYGULAMALARININ İNCELENMESİ

MEHMET GÜRKAN ÖZYAZICI

YÜKSEK LİSANS TEZİ

MALZEME BİLİMİ VE MÜHENDİSLİĞİ ANABİLİM DALI

DANIŞMANI
DOÇ. DR. EBRU MENŞUR ALKOY

GEBZE
2018

SUMMARY

Underwater SONAR (SOund Navigation And Ranging) systems, medical imaging systems etc. use piezoelectric ceramics materials. Lead Zirconate Titanate (PZT) is the most commercially used polycrystalline piezoelectric composition because of its relatively higher properties and higher Curie temperature, utilizing in a wide range of applications. In this study, the objective was to investigate relatively new polycrystalline piezoelectric materials used in some certain applications such as passive underwater listening, ultrasonic imaging. Some compositions in the literature were investigated in order to enhance the properties of the PZT ceramic. Lead Nickel Niobate (abbreviated as PNN) is one of the first known polycrystalline compositions as relaxor ferroelectric. In this study, producibility of PNN-PZT with advanced electrical properties was investigated in order to improve aforementioned device applications. However, bulk piezoceramics have low efficiency in underwater applications. As a result, piezocomposites with 1-3 connectivity was fabricated. Ceramic fibers were fabricated by alginate gelation route. 1-3 piezocomposites were manufactured from those ceramic fibers. It was aimed to the superior electromechanical properties PNN-PZT composition for these applications, manufacturing of its fibers with alginate gelation route and fabrication of 1-3 piezocomposites from those fibers for the first time. Two different fabrication methods (Mixed Oxide Route and Columbite Precursor Route) were investigated and X-ray diffraction results, SEM images, and electrical measurements were conducted for both routes comparably. Modelling by Finite Element Method of PNN-PZT composition were also investigated in this study. Hollow spherical hydrophones were also fabricated as a final device demonstration.

Keywords: Lead Nickel Niobate, Lead Zirconate Titanate, Alginate Gellation, 1-3 Piezocomposite, PNN-PZT, Hollow Spherical Hydrophone.

ÖZET

Sualtı SONAR sistemleri, medikal görüntüleme sistemleri vb. alanlarda piezoelektrik seramiklerden yararlanılmaktadır. Kurşun Zirkonat Titanat (PZT) görece yüksek özellikleri ve yüksek Curie sıcaklığı ile faklı alanlarda ticari olarak en yaygın şekilde kullanılan bir piezoelektrik kompozisyonudur. Bu çalışmada özellikle pasif sualtı dinleme cihazları, ultrason görüntüleme gibi uygulamalarda kullanılan polikristalin piezoelektrik kompozisyonların geliştirilmesi amaçlanmıştır. Bu tip uygulamalar için ticari olarak en yaygın şekilde bulunan PZT'nin özelliklerini geliştirmek amacıyla farklı kompozisyonlar literatürde araştırılmıştır. Kurşun Nikel-Niyobat (PNN) soft karakteristiğe sahip olup bilinen ilk relaxor ferroelektrik malzemelerden biridir. Bu çalışmada gelişmiş elektriksel özelliklere sahip PNN-PZT kompozisyonunun üretilebilirliği ve yukarıda belirtilen alanlarda kullanılacak cihaz uygulamalarının geliştirilmesi incelenmiştir. Ancak bulk halde üretilen piezoelektrik seramiklerin sualtı uygulamalarındaki performanslarının verimliliği düşüktür. Bu sebeple sualtı cihaz uygulamalarında verimliliği artırmak adına bu kompozisyondan 1-3 bağlantılı piezokompozit üretilmiştir. Fiberler alginate jelleşmesi yöntemi ile üretilmiştir. Elde edilen bu fiberlerden 1-3 bağlantılı piezokompozitler üretilmiştir. Bu çalışma ile PNN-PZT kompozisyonunun üstün elektromekanik özellikleri belirtilmek ve ilk defa alginate jelleşmesi yöntemi ile fiber halinde elde edip, bu fiberleri 1-3 bağlantılı piezokompozit halinde üretmek hedeflenmiştir. Çalışmada Oksitlerin Karışımı(Mixed Oxide) ve Kolümbit Öncül(Columbite precursor) yöntemi karşılaştırılmış ve her iki yöntem için de X-ışınları difraksiyonu sonuçları, Taramalı Elektron Mikrokobu(SEM) görüntüleri ve elektriksel ölçümleri alınmıştır. Ayrıca bu çalışmada PNN-PZT kompozisyonunun Sonlu Elemanlar Yöntemiyle modellenmesi incelenmiştir. Nihai bir aygıt uygulaması olarak içi boş küresel hidrofonlar da bu çalışma kapsamında üretilmiştir.

Anahtar Kelimeler: Kurşun Nikel-Niyobat, Kurşun Zirkonat Titanat, Alginate Jelleşmesi, 1-3 Piezokompozit, PNN-PZT, İçi Boş Küresel Hidrofon.

ACKNOWLEDGEMENT

First of all, I would like to start by stating my gratitude to my advisor Assoc. Prof. Ebru MENŞUR ALKOY for contributing to this thesis with her support, advises, encouragement as well as Prof. Sedat ALKOY for his help, support and advises during this thesis study. I am highly appreciated due to finding a chance to work with both of them.

One of the biggest thanks to my friend and my colleague M. Yunus KAYA who supported, advised and guided me during this study. I believe that I could not finish this study in this period without his help.

I would like to thank my friends, M. Ünsal ÜNVER, Merve TEBER, Mehmet AKSOY, Aycan KARAMAN, Gökhan GÜNAY, Anıl BOZDOĞAN, Kadir KOÇAK, Hüseyin Alptekin SARI, M. Yenal Yalçınkaya, Ayşe BERKSOY YAVUZ for their physically help and mentally support.

I also would like to express my gladness to my friends, Cemil Şan AKASLAN, Cihangir AKSOY, Nurcan YILDIRIM, Eftal GEÇGİL, Abdurrahman AKCAN and Cansu UĞURLUEL for always being around me and show their friendships.

I would like to thank Mr. Adem ŞEN and Mr. Ahmet NAZIM for their help anytime I needed.

I would like to thank Mr. Cem ÖZTÜRK whom financially supported me and who I found a chance to work with later on. I feel lucky to know him.

Lastly, the most special gratitude to my mother Nimet ÖZYAZICI, my father Ali Ekrem ÖZYAZICI, my sister Dilek ÖZYAZICI, my brother Okan ÖZYAZICI and to my dearest cousin Özlem BALO. I am very glad that I have them. They always supported me with my decisions in my life. I believe that I am a courage person with them.

This thesis was a part of the project financially supported by TÜBİTAK(Project #112M791, Project Director: Ebru MENŞUR ALKOY).

TABLE OF CONTENTS

LIST of ABBREVIATIONS and ACRONYMS

Abbreviations and Acronyms		Explanations
Z	:	Acoustic Impedance
Å	:	Angstrom
f_a	:	Anti-Resonance Frequency
C	:	Capacitance
E_c	:	Coercive Field
C	:	Coloumb
T_c	:	Curie Temperature
^oC	:	Degree Celcius
ρ	:	Density
Ø	:	Diameter
K	:	Dielectric Constant
tan δ	:	Dielectric Dissipation Factor
D	:	Dielectric Loss
χ	:	Dielectric Susceptibility
c	:	Elastic stiffness
D	:	Electrical Displacement
ε	:	Electrical Permittivity
$ε_0$	:	Electrical Permittivity of Vacuum
E	:	Electric Field
k	:	Electromechanical Coupling Factor
F	:	Force
Hz	:	Hertz
kHz	:	Kilohertz
Q_m	:	Mechanical Quality Factor
MPa	:	Megapascal
m	:	Meter
m^2	:	Meter square

μm	:	Micrometer
mm	:	Millimeter
min	:	Minute
MPB	:	Morphotropic Phase Boundary
Ω	:	Ohm
%	:	Percentage
pC/N	:	Picocoloumb per Newton
d_h	:	Piezoelectric Charge Coefficient
g_h	:	Piezoelectric Voltage Coefficient
P	:	Polarization
PVDF	:	Polyvinylidene Fluoride
PVDF-TrFE	:	Polyvinylidene Fluoride- Trifluoroethylene
Pr	:	Remanent Polarization
f_r	:	Resonance Frequency
Pp	:	Saturation Polarization
Ps	:	Spontaneous Polarization
SEM	:	Scanning Electron Microscope
~	:	Tilde
V	:	Voltage
wt	:	Weight
XRD	:	X-ray diffraction
$BaTiO_3$	:	Barium Titanate
$CaTiO_3$	:	Calcium Titanate
PSN-PT	:	Lead Scandia Niobate Titanate
PMN-PZT	:	Lead Manganate Zirconate Titanate
PZN-PT	:	Lead-Zinc Niobate Titanate
PNN-PZT	:	Lead Nickel Niobate Zirconate Titanate
NDT	:	Non-Destructive Testing
SONAR	:	Sound Navigation And Ranging

LIST of FIGURES

LIST of TABLES

1. INTRODUCTION

Smart materials and systems are capable of sensing changes in the environment where they are involved and response conveniently and accordingly [Newnham, 1991]. Piezoelectric materials can be called as “smart materials”. They have the ability to transform electrical input into mechanical displacement or acoustic output and reversibly, they can transform mechanical stress into electrical charge. Owing to this effect, these kinds of materials are used in underwater applications(such as SONAR), medical ultrasound devices and non-destructive testing(NDT) devices.

The first demonstration of piezoelectricity effect was made by Pierre and Jacques Curie brothers in 1880. This effect first found in single crystals such as tourmaline, Quartz, Rochelle Salt [Jaffe, 1971]. Afterwards, scientists started to study on polycrystalline compositions substitute for single crystals since they are not able to easily commercialize, because their production is difficult, expensive and it takes a long time. Hence, Barium Titanate ($BaTiO_3$) was discovered as the first piezoelectric and ferroelectric polycrystalline material. This material has good electrical properties, however, on the other hand, it has some limitations for applications. Jaffe et al. demonstrated that there is piezoelectricity in polycrystalline composition of Lead Zirconate Titanate (PZT) in 1954. Since then, PZT has become one of the most commercial piezoelectric ceramic materials which also exhibits ferroelectric property [Newnham et al. 1998], [Jaffe et al. 1954].

PZT is a normal ferroelectric material. In last decades, there has been an ascending relevance for piezoelectric and electrooptic materials in terms of high electrical performances. Relaxor ferroelectrics were discovered by Smolenskii in the late of 1950s. $Ba(Ti, Sn)O_3$, PMN, PZN are well-known relaxor ferroelectrics. Relaxor ferroelectrics have higher dielectric constants than normal ferroelectrics and they have diffuse phase transition [Uchino 2010]. Many various relaxor–ferroelectric based piezoelectric ceramic compositions have been developed to fulfill this demand. Some on-going studies are: $Pb(Sc_{1/2}Nb_{1/2})O_3$-$PbTiO_3$ (PSN-PT) , $Pb(Mg_{1/3}Nb_{2/3})O_3$-$PbZrO_3$-$PbTiO_3$ (PMN-PZT) , $Pb(Zn_{1/3}Nb_{2/3})O_3$-$PbTiO_3$ (PZN-PT) and $Pb(Ni_{1/3}Nb_{2/3})O_3$-$PbZrO_3$:$PbTiO_3$ (PNN-PZT) [Alberta, 2001].

1.1. Aim Of The Study

0.5PNN-0.35PT.0.15PZ system was selected and used for different potential piezoelectric applications. PNN-PZT is a relaxor-normal ferroelectric and in this study the first aim was to produce it and investigate its properties. The material has high electromechanical properties when compared to PZT. Two different methods, mixed oxide route, and columbite precursor route were used in this study. After obtaining electrical properties from bulk samples, PNN-PZT fibers were fabricated by alginate gelation route. Also, hollow sphere PNN-PZT ceramics were fabricated by slip casting method. Production methods were also investigated in order to optimize the properties of the composition. Modelling of the composition by Finite Elements Method(ATILA) were made on the purpose of confirmation of electromechanical measurement. The matrix of experimental results of PNN-PZT composition were also demonstrated in this study. Lastly, hollow spherical hydrophones were fabricated in the scope of this study.

2. LITERATURE REVIEW

2.1. Electroceramics

Ceramic materials can be divided into two major groups; conventional ceramics and electroceramics[Carter and Norton, 2007]. Conventional ceramics are mostly used as construction materials(brick, tile etc.). Electroceramics are mostly used in specific applications such as capacitors, transducers, thermistors etc. Discovering of new materials of electroceramics helps to develop micro-electro-mechanical applications [Carter and Norton, 2013]. Various of ceramics are used as an insulator under high and low electrical stress. Ionic and covalent bonds in ceramic materials, limit electron and ion movement within the material and this makes these materials good insulator [Smith W.F., 1990]. Electroceramics are such insulators since they have dielectric property. Due to this property, electroceramics are used in capacitor applications in cases where especially required very small areas in electronic circuits.

2.1.1. Dielectricity

There is no free current flow in dielectrics(or insulating materials) when they are applied an electric field. Because, unlike metals, dielectrics have no free electrons [Carter and Norton, 2007]. All materials contain electrically charged particles. Many ceramics also contains ions. In dielectrics, these ions have a limited movement which does not allow the electrical conduction in itself. And this limited movement can occur only when they have high enough energy. When dielectrics have an electrical charge, they hold this charge in some certain place in the material. However, conducting materials, allow the electrical charge replace freely through the material. To say so, the main difference between dielectrics(insulators) and conductors is that the mobility of electrical charge in the material [Uchino, 2000]. As mentioned above dielectrics do not conduct electricity, however, effected by an electrostatic field. Nevertheless, dielectric materials, don’t draw interest just with the insulating property but with high dielectric constant(K) [Carter and Norton, 2007].

Dielectric constant is a measurement which exhibits storage capacity of a material. And showed by the following expression:

$$D = \varepsilon E \tag{2.1}$$

Where, D: Electrical displacement (C/m^2), ε: Electrical permittivity (F/m) and E: Electric Field (V/m). Dielectric constant or relative permittivity can be expressed by the following equation;

$$K = \varepsilon / \varepsilon_0 \tag{2.2}$$

Where ε_0: Permittivity of vacuum (8.85×10^{-12} F/m). Dielectric displacement (D) is equal to total of all the charges which stored on the electrode and polarization (P, C/m^2);

$$D = \varepsilon_0 E + P \tag{2.3}$$

As a result of combining equation (2.1) and (2.3);

$$P = (K-1)\varepsilon_0 E = \chi \varepsilon_0 E \tag{2.4}$$

Where χ defined as dielectric susceptibility and proportional to charge/free charge. Dielectric susceptibility is a measurement of the capacity of polarizability for dielectrics. [Carter and Norton, 2007], [Newnham, 2005].

In ionic crystals, anions are attracted to the anode and cations to the cathode because of electrostatic interaction when an electric field is applied. And this interaction causes electric dipoles. This phenomenon is known as the electric polarization of the dielectric. These contributions may be sorted as electronic, ionic and dipole reorientation (Figure 2.1). The frequency of the applied electric field

determines which mechanism will contribute to the comprehensive polarization of the material [Uchino, 2000].

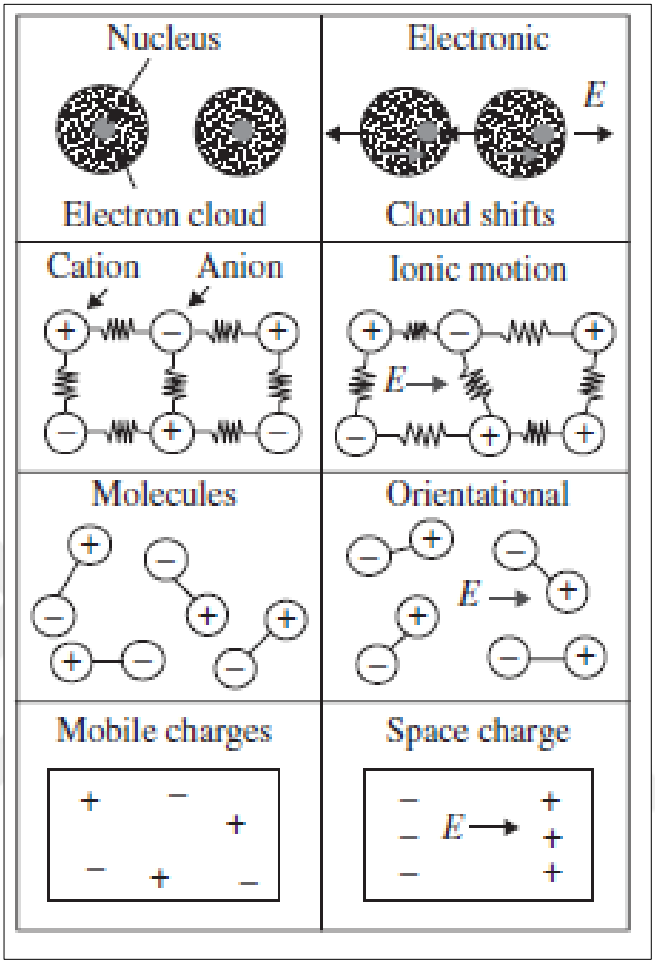

Figure 2.1: Polarization mechanisms under electric field.

Dipoles try to follow the direction of electric field. Dipoles reorient due to alternative current when another electric field is applied. Every polarization mechanism has a limiting characteristic frequency. Since electrons have to move consistently in more distance towards dipole reorientation, after a certain frequency, higher distance reoriented polarization mechanisms will be no longer effective. Only electronic polarization may be observed in higher frequencies(Figure 2.2) [Newnham, 2005]. In these frequencies, losses occur in dielectric materials since electrical energy transforms to heat [Newnham, 2005].

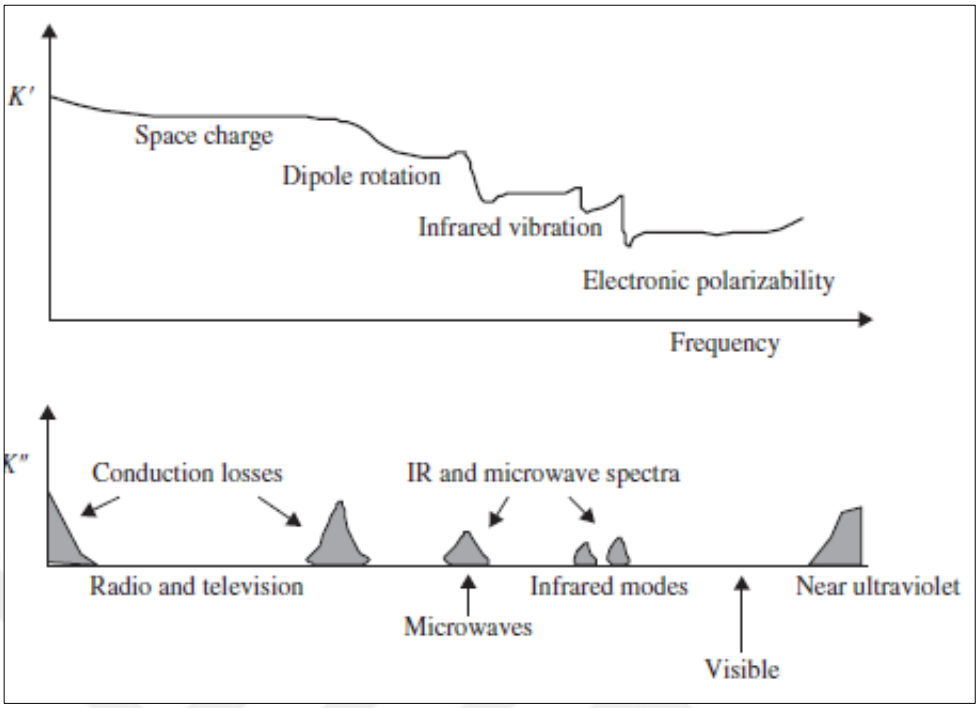

Figure 2.2: Dielectric spectrum of a dielectric material contains several polarization mechanisms.

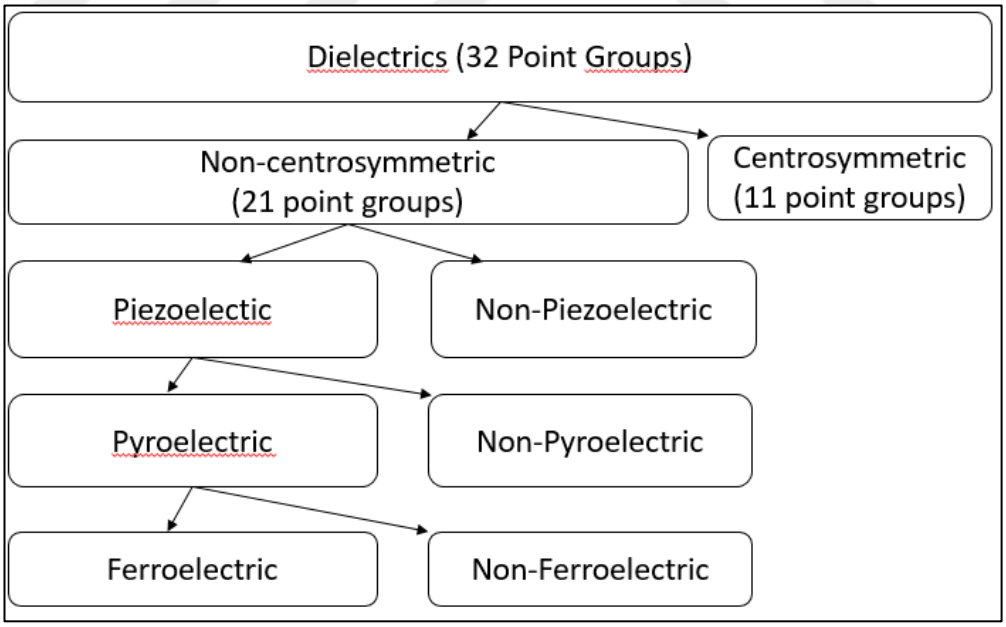

Figure 2.3: Calssification of dielectrics according to point group symmetries.

Some of the dielectrics which have non-centrosymmetric property exhibit piezoelectric property. Piezoelectric materials can have polarization as a result of

either applying an electric field or applying a stress to the material. Some of the piezoelectrics exhibit pyroelectric property which have spontaneous polarization and effect from temperature change. And some of the pyroelectrics exhibit ferroelectric property which have spontaneous and re-orientable polarization (Figure 2.3) [Kao, 2004].

- All ferroelectrics are pyroelectric and piezoelectric
- All pyroelectrics are piezoelectric
- All piezoelectrics are not pyroelectric.
- All pyroelectrics are not ferroelectric [Carter and Norton, 2013].

Dielectric dissipation factor (tan δ**);** is the tangent of dielectric loss in a material. tanδ is determined by the ratio of effective conductance to effective susceptance in a parallel circuit, measured by using an impedance bridge. This value is usually determined at 1 kHz. If tanδ is high then this means that there is a current flow through the material [www.americanpiezo.com].

2.1.2. Piezoelectricity

The piezoelectric property was found by Jacques and Pierre Curie in non-centrosymmetric single crystals such as quartz, tourmaline in the later of 18th century. They discovered this effect by applying mechanical stress. As a result of applied mechanical stress, charge accumulation is observed on the surface of the material. Word of "piezo" comes from Ancient Greek which means "pressure". Some certain materials accumulate electrical charge when they are applied a mechanical stress or they exhibit mechanical displacement when they are applied an electric field. This reversible effect called piezoelectric effect. Observing polarization in a material under mechanical stress is called direct piezoelectric effect. Observing mechanical displacement under applied electric field is called reverse piezoelectric effect [Haertling, 1999]. Piezoelectricity is seen in ilmenite structure as well as in perovskite structure[Matthias and Remeika, 1949]. However, it is possible to achieve large piezoelectricity with perovskite structure [Uchino, 2010].

In general, perovskite structure possesses ABO_3 formula. Where cations imply as "A" located in the center of large octahedron in fcc(face-centered cubic) structure. However, this is not the same for tetrahedron because of the charges. The ideal perovskite structure is simple cubic. If we look at $CaTiO_3$ mineral as an example of the perovskite structure, both large cation Ca^{2+} and relatively smaller Ti^{4+} have a bond with O^{2-} anion. Actually, this mineral has orthorhombic structure at room temperature and transforming cubic structure above 900°C.

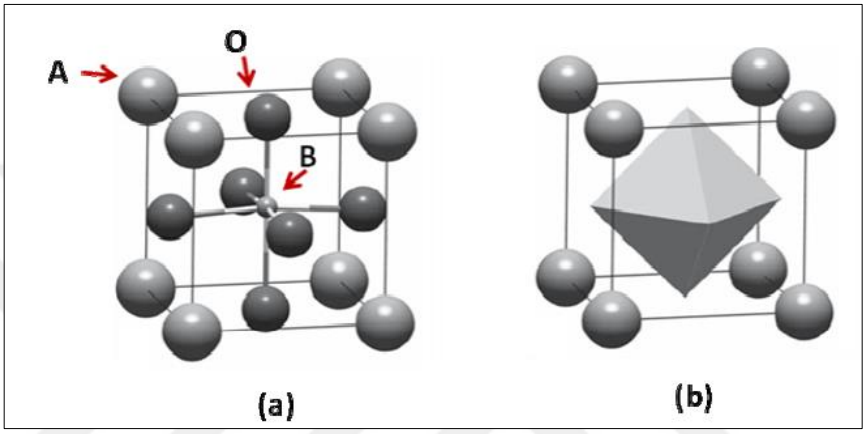

Figure 2.4: Perovskite crystal structure. Simple cubic crystal structure in which some cations occupy in the center of the octahedron. (a) Atomic model, (b) Polyhedron.

$BaTiO_3$ is a typical ferroelectric material which has perovskite structure above 120°C. When $BaTiO_3$ cools down below 120°C Ti^{4+} cation shifts a little bit. And this creates an electrical dipole, so the structure polarizes. This polarization makes the structure non-cubic by changing the dimensions. This means there is a spontaneous polarization in the absence of applied electric field which termed ferroelectricity which will be held in detail in the next parts.

Many perovskites are ferroelectric also piezoelectric and they have a high dielectric constant. These are some of the reasons why perovskite structures are important [Carter and Norton, 2013].

2.1.2.1. Piezoelectric Properties

Piezoelectric charge coefficient (d), can be described as obtaining a polarization as a result of applied mechanical stress to a material or obtaining a

mechanical strain(mechanical displacement) as a result of applying an electric field to per unit area. The first sub-index (d_{ij}) shows the direction of applied electric field force or the direction of polarization when an electric field is absent, and latter sub-index shows the direction of applied mechanical stress or induced mechanical strain. d constant is an important indicator for strain-dependent applications such as actuators. Directions are shown in Figure 2.5 [www.americanpiezo.com].

d_{33}; indicates stimulated polarization in direction 3 as a result of applied stress per unit into the direction 3 (parallel to polarization direction) or obtained strain per unit in direction 3 as a result of applied electric field per unit in direction 3.

d_{31}; indicates stimulated polarization in direction 3 as a result of applied stress per unit into the direction 1 (perpendicular to polarization direction) or obtained strain per unit in direction 1 as a result of applied electric field per unit in direction 3.

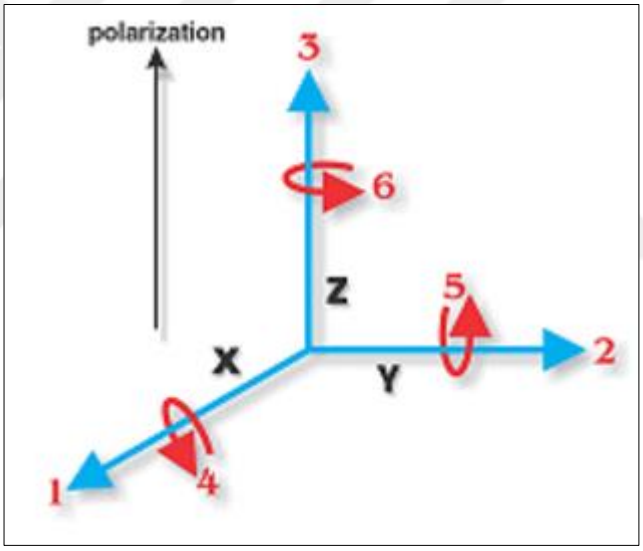

Figure 2.5: Directions of forces affecting a piezoelectric element

$$d = k\sqrt{(s^E \varepsilon^T)} \quad (2.5)$$

$$d_{31} = k_{31}\sqrt{(s^E_{11} \varepsilon^T_{33})} \quad (2.6)$$

$$d_{33} = k_{33}\sqrt{(s^E_{33} \varepsilon^T_{33})} \quad (2.7)$$

Piezoelectric voltage coefficient (g); can be described as obtaining an electric field as a result of applied mechanical stress to a material or obtaining a mechanical strain(mechanical displacement) as a result of applied unit electric field. The first sub-

index (g_{ij}) shows the direction of applied electric field force or the direction of electrical displacement, and latter sub-index shows the direction of applied mechanical stress or induced electrical strain. g constant is an important value which shows whether the materials is suitable for sensor applications.

g_{33}; indicates stimulated electrical displacement in direction 3 as a result of applied stress per unit into the direction 3 (parallel to polarization direction) or obtained strain per unit in direction 3 as a result of applied electric field per unit in direction 3.

g_{31}; indicates stimulated electric field in direction 3 as a result of applied stress per unit into the direction 1 (perpendicular to polarization direction) or obtained strain per unit in direction 1 as a result of applied electrical displacement per unit in direction 3 [www.americanpiezo.com].

$$g = d / \varepsilon^T \tag{2.8}$$

$$g_{31} = d_{31} / \varepsilon^T_{33} \tag{2.9}$$

$$g_{33} = d_{33} / \varepsilon^T_{33} \tag{2.10}$$

2.1.2.2. Electromechanical Properties

Electromechanical Coupling Factor (*k*); indicates the effectiveness of power of piezoelectric effect, so that it is a measurement of transformation electrical energy into mechanical energy or mechanical energy into electrical energy.

$$k_{eff}^2 = \frac{Stored\ mechanical\ energy}{Input\ electrical\ energy} \tag{2.11}$$

or

$$k_{eff}^2 = \frac{Stored\ electrical\ energy}{Applied\ mechanical\ energy} \tag{2.12}$$

Electromechanical transformation cannot be fully completed due to energy loss. For instance, *k* values are 0.1 for quartz, 0.4 for $BaTiO_3$, 0.7 for PZT and 0.9 for Rochelle Salt [Kao. 2004].

High k value usually desirable for efficient energy transformation, however, k does not account for either dielectric losses or mechanical losses. The total value of transformation is calculated by the notation above and it implies transformation proportion. This value can reach up to 90% for a good designed piezoelectric ceramic. k_p is planar coupling factor for thin disc piezoelectric ceramic materials.

Thickness coupling factor for the ceramic discs where surface dimensions are large relative to thickness is k_t. And k_{33} expressed the mechanical vibration in direction 3 with applied electric field in the same direction.

- k_{33}; expresses the electric field in direction 3 and longitudinally vibration in direction 3. This is for ceramic rods whose length is 10 times bigger than it's diameter.
- k_t; expresses the electric field in direction 3 and longitudinally vibration in direction 3. This is for thin discs ($k_t > k_{33}$)
- k_{31}; expresses the electric field in direction 3 and longitudinally vibration in direction 1. This is for ceramic rods.
- k_p; expresses the electric field in direction 3 and radial vibrations in direction 1 and direction 2. This is for thin disks [www.americanpiezo.com].

Mechanical quality factor (Qm), is the proportion of reactance to resistivity in a material. This method is used in order to determine the resonance properties of piezoelectric, and also to measure the impedance depending on frequency. The impedance of piezoelectric material passes at the minimum at resonance frequency(fr) and passes at the maximum at anti-resonance frequency(fa). (Fig. 2.6). Piezoelectric material behaves as a capacitor when below resonance frequency and above anti-resonance frequency while it behaves as inductive between those frequencies. Mechanical quality factor(Qm), defines the quality of the piezoelectric material as vibration element and used to determine the sharpness of resonance peak. As mechanical quality factor value increases, the peak gets sharper [Jordan and Quanies 2002].

$$Q_m = \frac{f_a^{\ 2}}{2\Pi C Z_m f_r (f_a^2 - f_r^2)} \tag{2.13}$$

- f_r: Resonance frequency (Hz)
- f_a: Anti-resonance frequency (Hz)
- Z_m: Impedance at resonance (Ω)
- C: Capacitance (F)

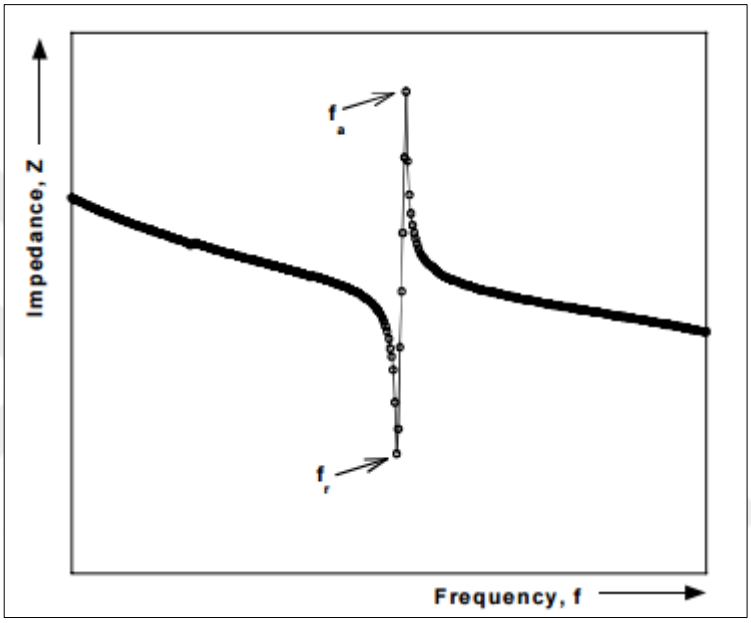

Figure 2.6: Typical impedance curve for resonance frequency measurement.

2.1.3. Ferroelectricity

The ferroelectric phenomenon is one of the most interesting properties of dielectrics. Materials which have reorientable spontaneous polarization are termed ferroelectric materials. These materials can be polycrystalline as well as single crystal. In normal dielectrics, polarization which is induced by an external electric field is very small (dielectric constant is mostly less than 100), however, in ferroelectric materials this constant can reach up to 10^4. Ferroelectric property can be defined as spontaneous polarization in the absence of applied electric field which can be reoriented under an applied electric field and limited with a transition point in some certain temperature called as Curie Temperature (T_c). The material loses its ferroelectric property above

T_c and behaves as normal dielectric material. Ferroelectric materials exhibit nonpolar behavior above T_c and especially near below T_c they have very high dielectric constant [Kao, 2004].

Ferroelectric property can be seen in some certain polymers such as polyvinylidene fluoride(PVDF) which has semicrystalline structure, and also some certain ceramics. Ferroelectrics form from regions which are called “domains”. Each domain has a polarization in different directions. Mostly there is almost no total net polarization since volumes of these domains nearly equal to each other [Carter and Norton, 2007].

In figure 2.7 [Kao, 2004], typical ferroelectric hysteresis loop is shown. In the loop, polarization increases with the increased electric field (A-B), then polarization saturates after a certain value of electric field (B-C). When electric field decreases, polarization mechanism follows C-B-D route. D value represents remnant polarization (P_r) which is the polarization value of the material when there is no more electric field. If electrcic field decreases (or increases in the reverse direction) polarization decreases (D-R). At point R, there is no polarization in the material even if there is an applied electric field. This is beacuse domains switch in the reverse direction along with the electric field. This point is called coercive field (E_c). R-G represents the polarization mechanism in the reverse direction. H shows remnant polarization in the reverse direction [Kao, 2004].

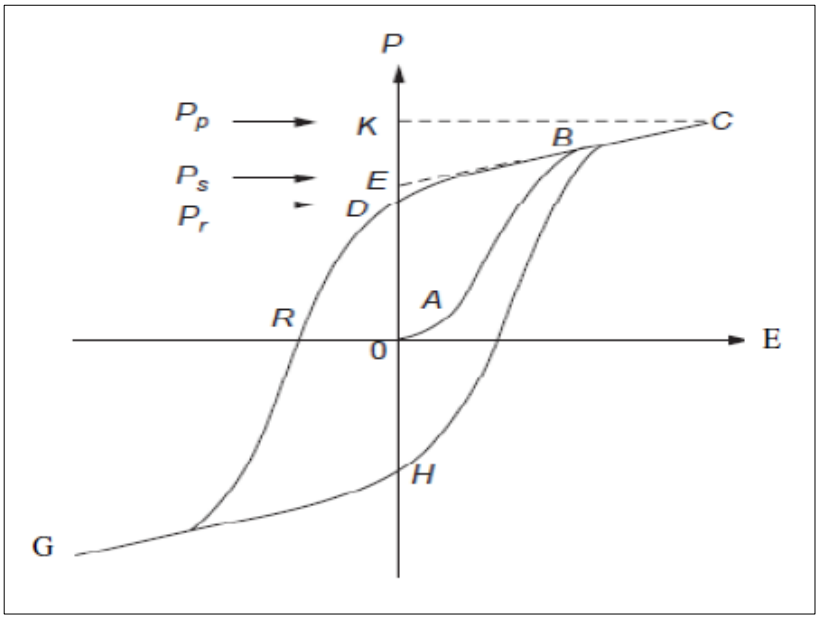

Figure 2.7: A typical ferroelectric hysteresis loop.

In general, four different ferroelectric ceramic materials. These are divided by their unit cell structures.

- Tungsten bronze structure
- Perovskite structure with oxygen octahedra (ABO_3)
- Pyrochlore structure
- Bismuth layered structure

The first found ferroelectric materials have ABO_3 perovskite structure. This structured ferroelectric ceramics the most using in applications and have the most market share group. Barium titanate ($BaTiO_3$), lead-zirconate-titanate(PZT), sodium-potassium niobate $(Na,K)NbO_3$ compositions are such commercially manufacturing ferroelectric materials. There are two types of ferroelectrics in the literature. Normal ferroelectrics and relaxor ferroelectrics. Relaxor ferroelectrics have disordered structure while normal ferroelectrics have ordered structure (Fig. 2.8) [Uchino, 2000]. And relaxor ferroelectrics are interesting for some certain applications due to their high dielectric and diffuse phase transition property [Uchino, 2010].

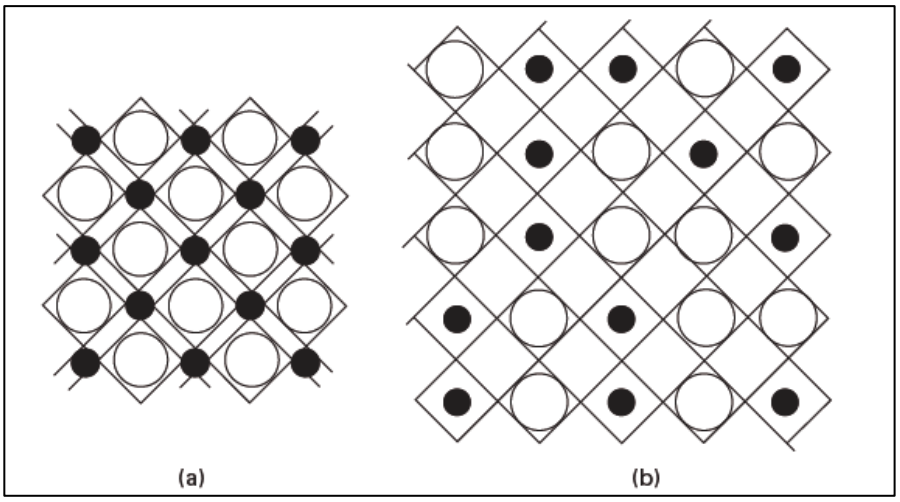

Figure 2.8: Crystal structure models of the $A(B_{I,1/2}B_{II,1/2})O_3$-type perovskite structure. B_I(empty) is lower valence cation, and B_{II}(filled) is higher valence cation. a) Ordered structure b) disordered structure

2.1.3.1. Relaxor Ferroelectrics

Relaxor ferroelectrics are utilized highly in capacitors. The reason that utilizing is that they have a high relative permittivity, diffuse phase transition, and high piezoelectric coefficient.[Damjanovic, 1998]. Since they possess diffuse phase transition they do not have a certain Tc (Curie temperature), unlike normal ferroelectrics. And this Tc moves proportionally to the frequency[L.E. Cross, 1987]. Figure 2.9 shows relaxor and normal ferroelectrics dielectric behaviour against temperature and frequency in comparison [Uchino, 2010].

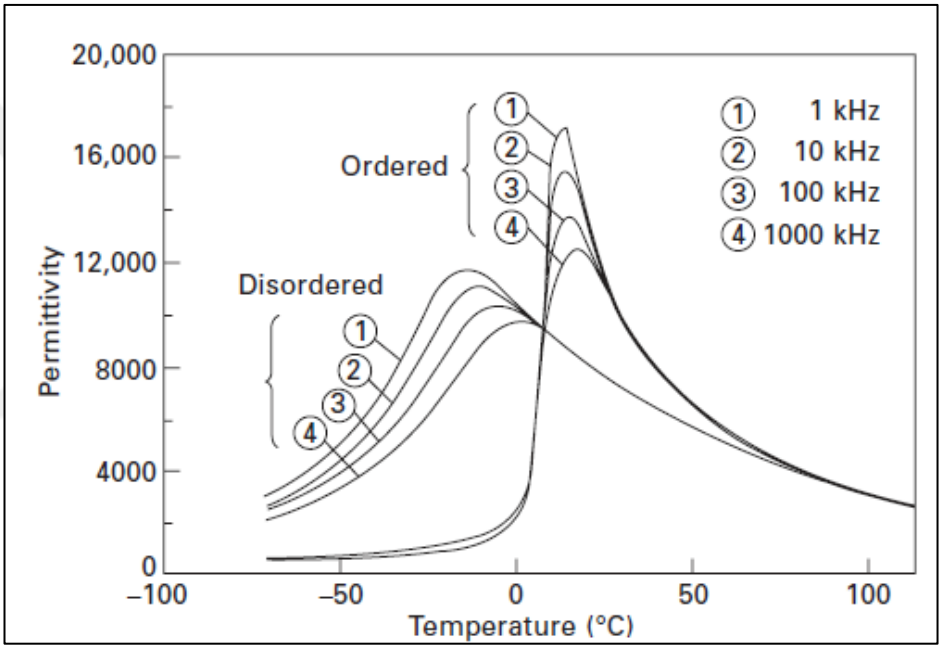

Figure 2.9: Frequency dependence of Curie Temperature(T_c) in ordered and disordered structures.

This phenomenon based on its structure. Relaxor ferroelectrics have disordered perovskite structure while normal ferroelectrics have ordered perovskite structure. There are two sizes of atoms basically (large and small sizes). In normal ferroelectrics, small ions have limited place to move. However, small ions have more space to move within structure in relaxor ferroelectrics. Because large ions cause to open the lattice frame. This movement of small ions in relaxor ferroelectrics puts them in an important position for memory device application [Uchino, 2000].

2.2. Polycrystalline PNN-PZT

In 1958, Lead nickel niobate [$Pb(Ni_{1/3}\ Nb_{2/3})O_3$, PNN], which has a soft characteristic, was discovered by Smolenskii and Agranovskaya as a single crystal in 1958. PNN also is known as one of the first relaxor ferroelectrics which has a cubic prototype symmetry Pm3m with (a)=4.03 Å lattice parameter proved by Bokov and Mylnikova in 1961 [Vittayakorn, 2004], [Damjanovic, 1998].

PNN consist of lead oxide (PbO), nickel oxide (NiO) and niobium oxide (Nb_2O_5). Ni^{2+} is divalent and Nb^{5+} is pentavalent cations, $Ni^{2+}$and Nb^{5+} accommodate on B site in the perovskite structure.[Randall 1990]. PNN has -120^oC Tc and relative permittivity near 4000 at 1 kHz [Vittayakorn, 2004].

PZT consist of lead oxide (PbO), zirconia(ZrO_2) and titanium oxide (TiO). Zr^{4+} and Ti^{4+} are tetravalent cations. Demanded properties can be achieved by adjusting compound percentages and microstructures [Carter and Norton, 2007]. PZT is a normal ferroelectric and PNN is relaxor ferroelectric. Normal-relaxor ferroelectric composition PZT with high Tc(Curie Temperature) and PNN with high piezoelectric coefficient is used in literature [Vittayakorn, 2004].

In 1965, the first PNN based polycrystalline system $Pb(Ni_{1/3}\ Nb_{2/3})ZrTiO_3$ (PNN-PZT) was investigated by Buyanova et al. They studied the effect of Morphotropic Phase Boundary (MPB) for this composition. In 1974, the more enhanced study was carried out by Luff et al. for PNN-PZT composition. Luff et al. reached excellent electrical properties with the composition $0.5Pb(Ni_{1/3}Nb_{2/3})O_3$-$0.35PbTiO_3$-$0.15PbZrO_3$ (d_{33}=1100 pC/N) [Vittayakorn, 2004]. PNN-PZT phase diagram was given in Fig 2.10[Bove et al., 2001].

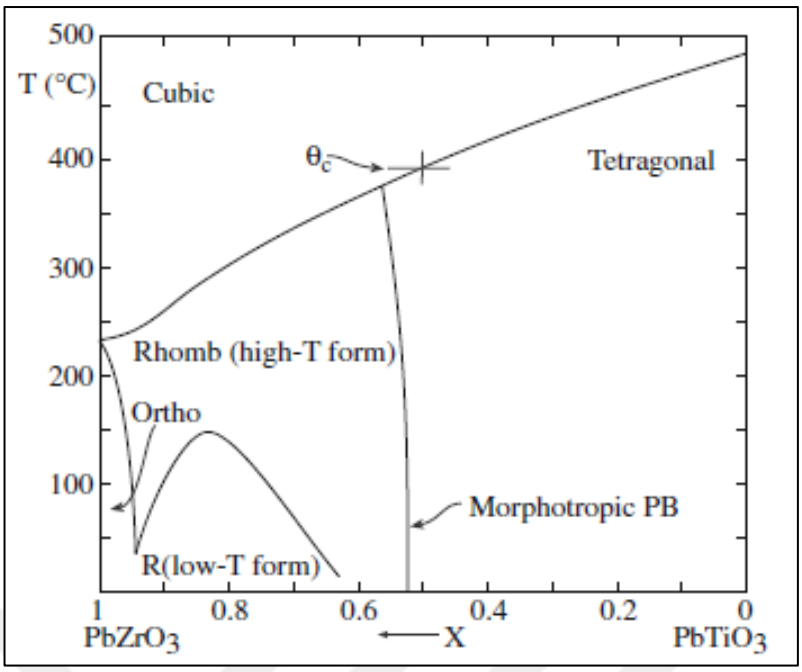

Figure 2.10: Phase Diagram of PZT.

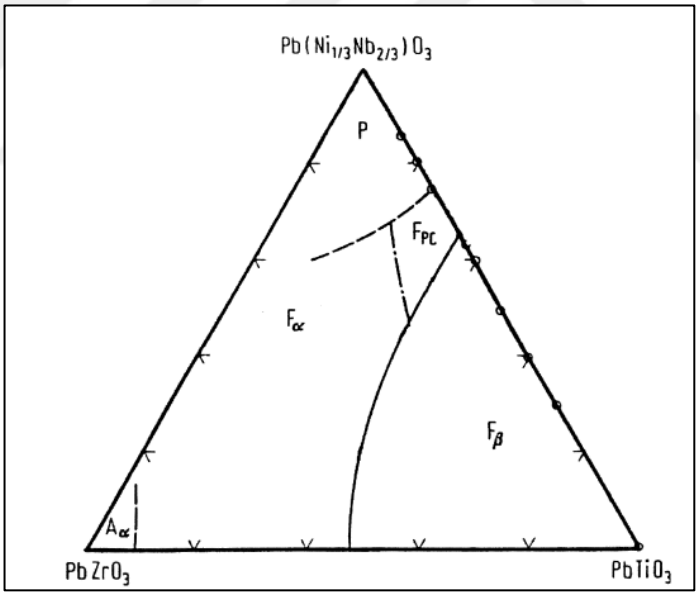

Figure 2.11: Phase diagram of PNN-PZT system. Where F_α is rhombohedral, F_β tetragonal, F_{PC} pseudocubic, P cubic paraelectric, A_α antiferroelectric phase.

2.3. Electroceramic Composites (Electroceramics)

Ferroelectric materials are not commercially used only for their ferroelectric properties in applications, however, they are also used with their high piezoelectric properties. Lead zirconate titanate (PZT) solid solution is the most commercially used

piezoelectric material in underwater acoustic(SONAR, hydrophone etc.) or medical imaging applications [Newnham, 1994]. However, low susceptibility and high acoustic resistance of bulk PZT, and additionally, low hydrostatical piezoelectric charge coefficient (d_h) and voltage coefficient (g_h) limit utilization of bulk PZT for these kinds of applications. Hydrostatical piezoelectric coefficient can be expressed as the following equation;

$$d_h=d_{33}+2d_{31} \tag{2.14}$$

d_{31} value is almost the half of d_{33} and has opposite sign of d_{33} for PZT, therefore d_h value for PZT is very low. Equation between g_h and d_h values are given below,

$$g_h=d_h/\varepsilon_{33} \tag{2.15}$$

In this equation, gh value is very low as well, because PZT has low dh and high ε_{33}(dielectric permittivity) value. For these reasons, hydrostatic "Figure of Merit" ($d_h x g_h$) will be low [Klicker et al., 1979], [Gururaja et al., 1994]. Besides, there is low acoustic harmony between material and propagating medium(water, human body etc.) for ultrasonic waves which created from bulk piezoelectrics. To overcome this disharmony by decent designing, there are some polymers which show the piezoelectric property. Most common ones are polyvinylidene fluoride (PVDF) and polyvinylidene fluoride-trifluoroethylene (PVDF-TrFE). These are expensive to produce and also they have a low dielectric coefficient, so they are limited to use [Janas et al., 1994].

Thus, in many applications, to overcome these disadvantages of piezoelectrics such as bulk PZT, composite materials, which include two different phases, one passive and one active, have developed [Newnham, 2004].

In the later 1970s, Newnham et al. proved that this problem in bulk piezoceramics can be overcame by a suitable connectivity of piezoelectric ceramics(active phase) and polymers(passive phase) [Newnham, 1978]. Hereby, in 1980s promising composite designs were developed for ultrasound transducers. Features on demand were obtained by adjusting distances between each active phases, volume fraction, and connectivity of active/passive phases. By these designs, figure of

merit of hydrophones for underwater applications are increased by decreasing the d_{31} value of the system [Wersing, 1986], [Smith, 1992].

In a piezoelectric composite, aligning of active and passive phases effect electromechanical properties, and thus, architectures of piezocomposites Newnham et al. were developed a systematic code for different phases. White color symbolizes the active phase and black color symbolizes the passive phase [Skinner, 1978]. As shown in Figure 2.8, there are 10 different connectivities in where every phase can have zero, one, two and three continuous connectivity in a system includes 2 phases in it [Pilgrim et al., 1987].

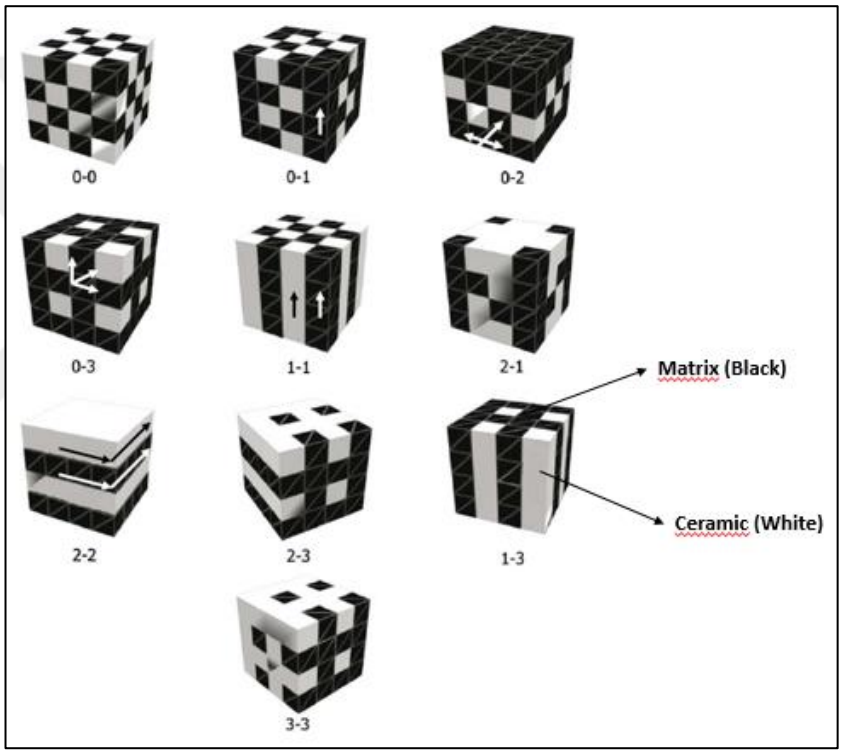

Figure 2.12: 10 different connectivity of which 2 phases composites can have.

(0-0), (0-1), (0-2), (0-3), (1-1), (1-2), (2-2), (1-3), (2-3) and (3-3) are accepted terminology to determine piezocomposites(Figure 2.12) [Heywang et al. 2008]. In this notation, the first number in parenthesis represents the degree of freedom for active phase and a second number represents for the passive phase in the composite. For instance, (1-3) composite indicates that piezoelectric ceramics are continuous in one direction and these ceramics are surrounded by a passive phase(i.e epoxy) which are continuous in 3 directions.

From PZT ceramics in polymers mostly 0-3, 2-2 and 1-3 connectivities are designed as piezocomposites. Because of many reasons, commercially utilized of these connected piezocomposites are preferred instead of conventional electroceramics. Some of them are;

- Piezocomposites get more suitable for water and human tissue with decreasing acoustic impedance as against to conventional ceramics.
- They act as acoustic insulating for adjacent transducer elements.
- Exhibit advanced susceptibility for hydroacoustic waves.
- They can absorb the active and passive vibrations.
- They can work at very high frequencies.
- They exhibit strength against to mechanical and electrical breakdown[Newnham, 2004].

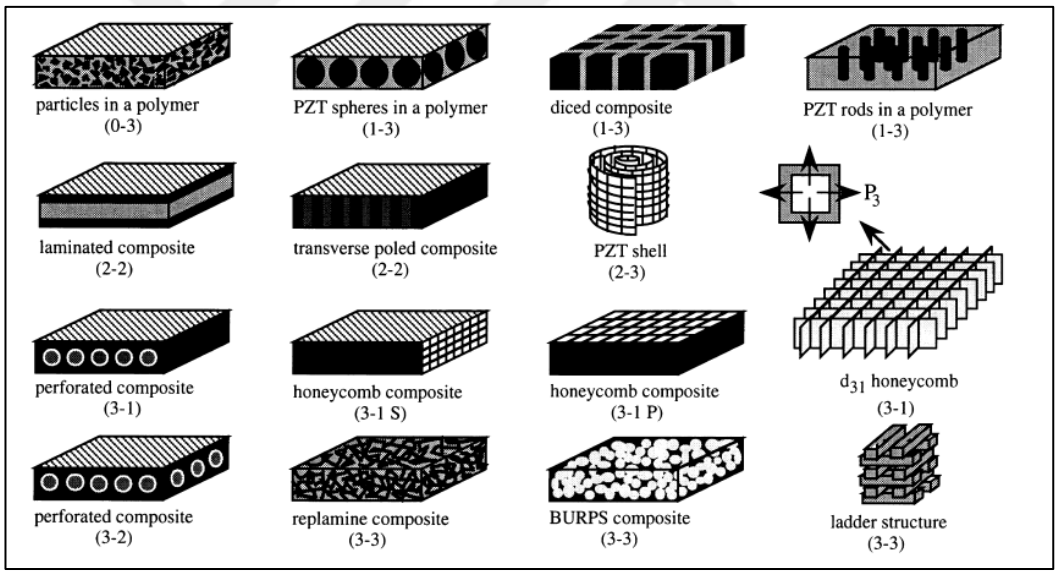

Figure 2.13: Different models of ceramic-polymer piezocomposites with different types of connections.

Figure 2.9 shows commonly used and commercialized 1-3 connected piezocomposite. PZT fibers are commonly used for 1-3 piezocomposites since they have designed because of their high piezoelectric properties as an active ceramic phase.

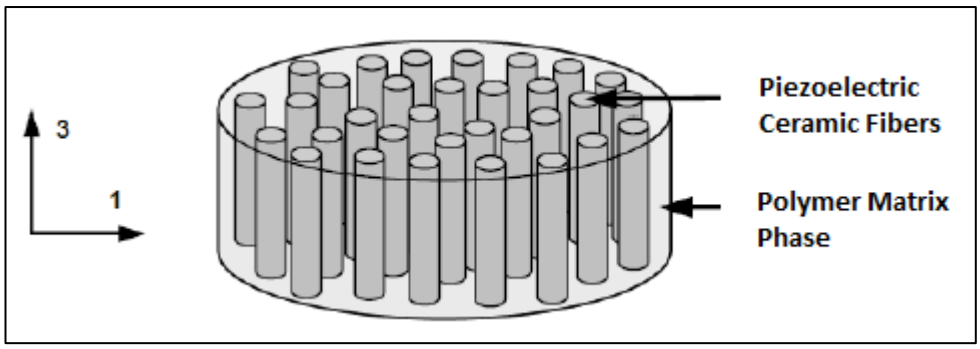

Figure 2.14: Schematic picture of 1-3 piezocomposite

Acoustic Impedance (Z), is a product of the density of medium and propagating of sound velocity in the medium. The unit for acoustic impedance is kg/m^{2}sec (so-called Rayl) reflection and transmission of acoustic signals at an interface between two different media is an important point of this phenomenon [Gururaja, 1994].

It is expressed by the following in general,

$$Z^2=\frac{Pressure}{Volume\ Velocity} \tag{2.16}$$

In solid materials, ρ

$$Z = \sqrt{\rho c} \tag{2.17}$$

Where ρ is the density and *c* is the elastic stiffness.

Thus when acoustic waves try to transmitted from one medium to another, some of those waves will reflect from the interface and will not pass through the interface, only the rest will pass through it. Although this makes us display the structure of the medium, also causes loss of signal resistance while it passes through the transducer. Therefore, the similarity between piezoelectric element and media is demanded. For example, the characteristic acoustic impedance of PZT approximately 35 MRayl, this is 3,4 MRayl for PVDF [Gururaja, 1994].

2.4. Piezoelectric Ceramic Fiber Production By Alignate Gelation Method

There are three basic routes for the production of ceramic fibers used in where 1-3 piezocomposites. These are extrusion, viscous suspension spinning, and sol-gel route. In addition to those routes, there is another effective route for fabricating of ceramic fibers termed alginate gelation route. Alkoy et al., fabricated electroceramic fibers by injection method from ceramic suspension. As a result, they achieved uniform ceramic PZT fiber with 200-300 μm diameters. [Alkoy,2007].

Sodium alginate has a natural structure because it is obtained from seaweed. It is water-soluble which can be gelated right after reacts with a divalent metal ion such as Ca^{2+}. Alginate is utilized in ceramic forming such as dry molding, extrusion, slip casting and stabilizing of suspension, and dry and wet strength. Also, it is utilized in gel casting, tape casting, and free solid shaping without mold. The best advantage of this process is that it provides strength while forming of the wet sample.

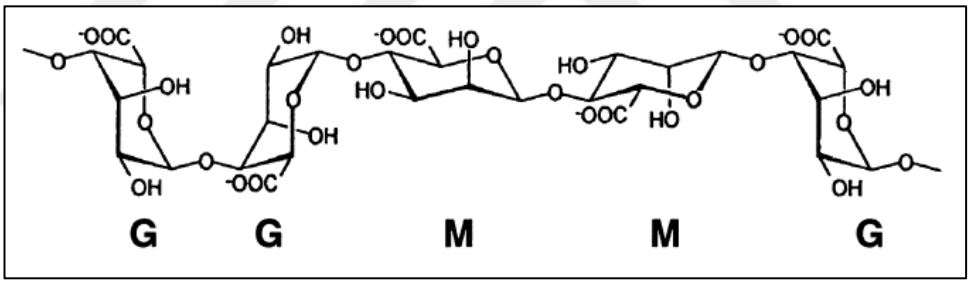

Figure 2.14: Structure of alginate copolymer.

Gelation of Sodium (Na) Alginate in the presence of Ca^{2+} ions takes place as given chemical formula below,

$$2\text{Na-alginate} + Ca^{2+} \leftrightarrow \text{Ca-alginate} + 2Na^{+} \quad (2.18)$$

As replacing of Ca^{2+} and Na^{+} ions, a 3-dimensional network forms with crosslinking of linear polymers and this prompts to the green ceramic has a form with ceramic particles hold on to this polymer network. Linking reactions can be varied depending on the amount of calcium and a chelating agent. This is important in terms of control of gelation behavior in gel-casting or ceramic forming processes. In addition

to this, high gelation rate in fiber production with injection method is very important in terms of protection of fiber forms which are injecting into the $CaCl_2$ solution. [Alkoy, 2007] [Jia et al., 2002].

2.5. Production of Hollow Spherical PNN-PZT Ceramics

Bulk piezoceramics have low efficiency in underwater hydrophone applications in terms of their impedance mismatching. In order to overcome this issue different designs were developed. For some applications hollow spherical transducers are used commonly. [Alkoy et. al., 1999]. The advantage of spherical transducer is that it can send and detect acoustic signal with 360^o angle. In order to overcome impedance mismatching, spherical transducers coating with polymer. Hollow ceramics from PNN-PZT was produced in order to fabricate a hydrophone transducer. Hemispherical hollow PNN-PZT ceramics were fabricated by slip casting method. Then hemispherical hollow ceramics were assembled to make a hollow spherical transducer, and lastly coated with polyurethane in this study.

3. EXPERIMENTAL STUDY

3.1. Powder And Bulk Sample Processing

Raw materials used in this study are Lead Oxide(PbO), Zirconium Oxide(ZrO_2), Titanium Oxide(TiO_2), Nickel Oxide (NiO) and Niobium Oxide (Nb_2O_5). Detailed information about the chemicals were given in the Table 3.1.

Table 3.1: Raw materials used for powder synthesizing.

Raw Material	Purity	Brand
PbO	99.9%	Alfa Aesar
ZrO_2	99+%	Alfa Aesar
TiO_2	99.5%	Alfa Aesar
NiO	99%	Alfa Aesar
Nb_2O_5	99.5%	Alfa Aesar

Two different fabrication methods were used in this study; Mixed oxide route and Columbite precursor route. Columbite precursor route was chosen, because, having perovskite structure can be difficult to obtain by mixed oxide route with relaxor ferroelectrics such as PNN in relaxor-normal ferroelectric compositions. The reason of this difficulty is Niobium is an effective pyrochlore former [Damjanovic et al. 2001].

Powders were ball-milled by using yttria-stabilized zirconia(YSZ) balls in the bottle for 24 hours. YSZ balls with 3 and 5 mm diameters were used in this study. Ethanol was used as milling carrier media. After drying process, the powders were calcined. Before the calcination process, in order to compensate Lead loss, 1 wt% excess PbO was added and before the sintering process 1 wt% excess PbO was also added for the same purpose.

First of all, powders were fabricated by mixed oxide route. In this method, raw ceramic powders were mixed together. After ball-milling and drying processes, they were calcined at 1000^{o}C for 4 hours with 5^{o}C/min heating rate. Binder was added to the synthesized powder and bulk disc-shaped ceramic samples were prepared by uniaxial pressing under 150 MPa, and they were sintered at 1200^{o}C for 4 hours. The processing flowchart was given in Figure 3.1.

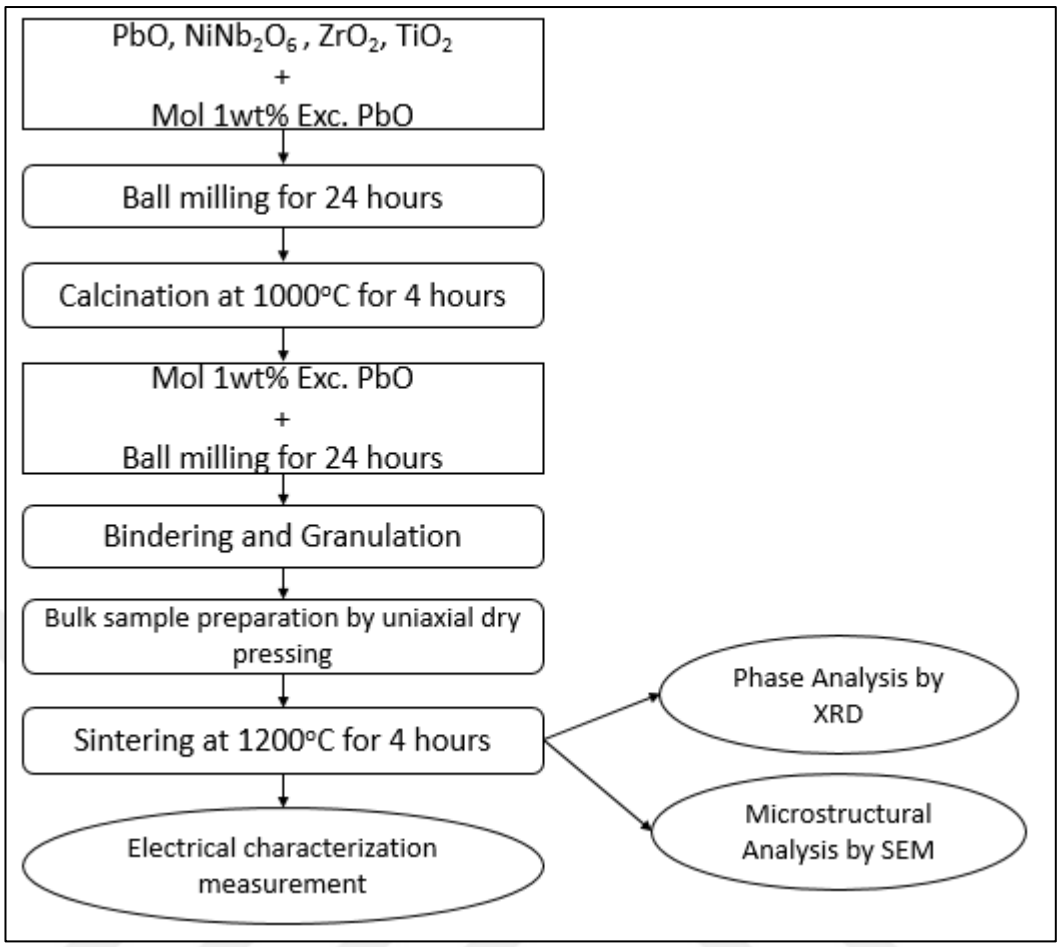

Figure 3.1: Flow chart of ceramic sample fabrication with mixed oxide route.

Secondly, powders were prepared by columbite precursor route. In this method, NiO and Nb_2O_5 are mixed and ground together. After mixing and drying process, the powders were calcined at 1100ºC for 4 hours.

$$NiO + Nb_2O_5 \rightarrow NiNbO_6 \quad (3.1)$$

$NiNbO_6$ and rest of the powders were mixed and ground together. And then all the powders were calcined at 1000ºC for 4 hours.

Before pressing binder was added. Bulk ceramic samples were prepared by uniaxial press again. They were sintered at 1200ºC for 4 hours.

Different sintering temperatures were also investigated. SEM images, P-E(polarization-electric field) and S-E(strain-electric field) for the temperatures 1100ºC, 1150ºC, 1200ºC and 1250ºC were also given in results.

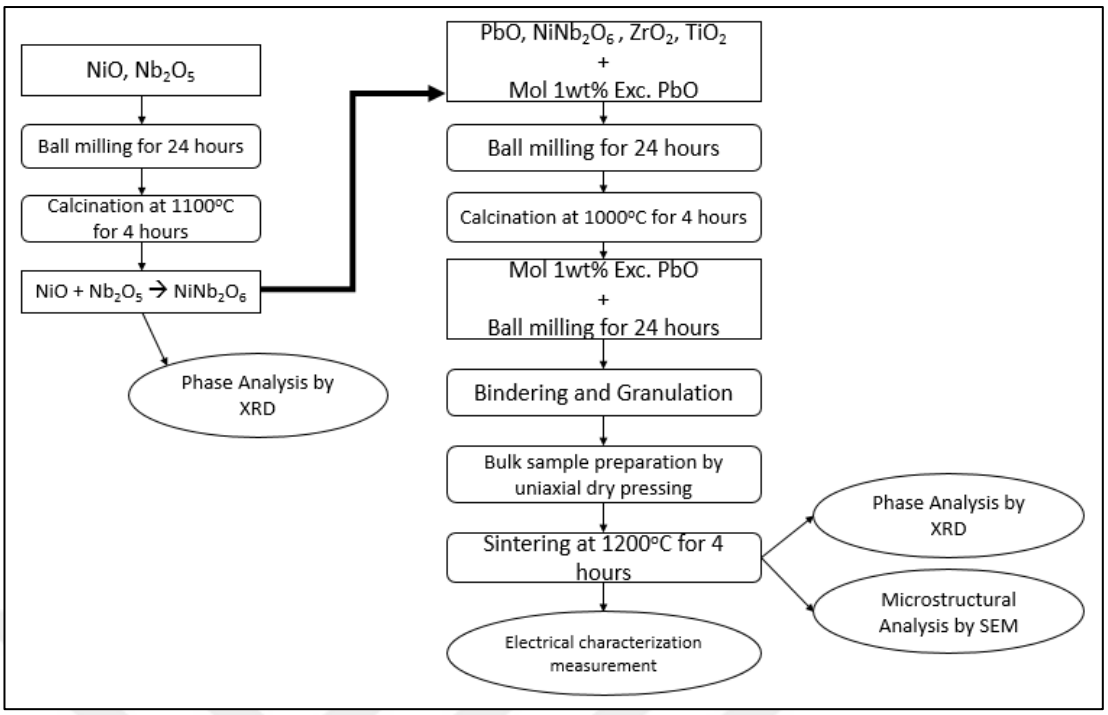

Figure 3.2: Flow chart of ceramic sample fabrication with columbite route.

Samples were prepared with 10 mm diameter and 1 mm thickness. Before sintering process, binder burned out process was carried out.

3.2. Fiber and Composite Processing

Fibers were prepared by alginate gelation route. Raw materials mixed together with a mechanical mixer. Ceramic slurry was mixed for 24 hours. Then the fibers were drawn by in-house fiber machine in the laboratory. For fiber fabricating process, powders produced by columbite route were chosen.

Table 3.2: Intended use of materials for alginate gelation route.

Raw Material	**Intended Use**
PNN-PZT Powder	Ceramic Compound
Alginic Acid	Gelation Agent
Distilled Water	Medium
Glycerol	Plasticizer
Darvan	Dispersant

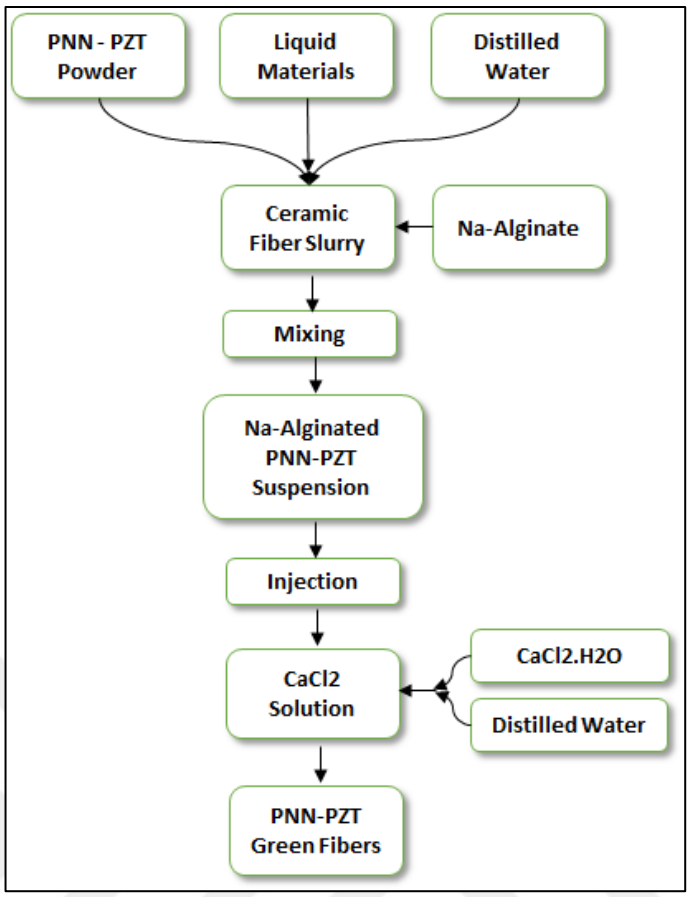

Figure 3.3: Flow chart of the ceramic fiber fabrication process.

$CaCl_2$ + distilled water was prepared with mixing until $CaCl_2$ solutionized completely. Afterward, ceramic slurry was injected into $CaCl_2$ solution. The diameter of the injection needle was 2 mm. Ceramic fibers were gelated fastly owing to this Na-alginate gelation method [Alkoy, 2007]. In order to confine the ceramic particles to form a consolidated green body, fibers kept into the $CaCl_2$ solution for 24 hours. Obtained green fibers hung in order to dry in air. After that dried ceramic fibers were sliced as 3 cm length and placed in an alumina crucible. Ceramic fibers were sintered at 1200^oC for 4 hours. In order to prevent lead loss during the sintering process, in spite of adding 1 wt% excess PbO to ceramic slurry, a bit of $PbO\text{-}ZrO_2$ atmosphere powder was also placed in an alumina crucible in which samples placed into together. Flowchart for ceramic fiber fabrication process was given in Figure 3.4.

After ion exchange of Ca and Na in the process, all the organics can be removed from the structure by binder burn-out process. However, Ca ions remain in the structure as a dopant on Pb-site. This may effect the electrical properties of the composition [Alkoy et al., 2007].

Piezocomposites with 1-3 connectivity were produced with the fibers which were obtained by alginate gelation route. Sintered ceramic fibers with 20 mm length were aligned in one direction with the help of two sliced metal wire cloth with a certain geometry. After having these aligned ceramic fibers, piezocomposites with 1-3 connectivity were prepared. The ceramic fibers placed into a mold and the empty spaces were filled by polyurethane. The polyurethane was vacuumed before adding to the ceramics as a matrix in order to avoid bubbles inside the matrix which causes a damage for electrical properties. In this system, sintered ceramics act as an active phase, and polyurethane acts as a passive phase [Newnham et al. 1998]. The composite system was waited for 24 hours in order to get samples dry. Then composites were sliced into different thicknesses.

Fiber fabrication was carried out with electrical driven fiber injection machine (MSE Technology, Turkey).

Figure 3.4: Fiber Injection Machine (MSE Technology) at Gebze Technical University Materials Science and Engineering Laboratory.

3.3. Structural Analyses

Phase analyses of the powders, fibers and bulk samples after calcination and sintering were done by X-ray diffraction method. Microstructures of both fabricated bulk and fiber samples were also examined by Scanning Electron Microscope(SEM).

3.4. Electrical Characterization

In accordance with the purpose of having flat surface and desired certain thickness, SiC sandpaper (English Abbresives) with numbers 800 and 1200 were used respectively.

The surfaces of the samples must be conductive to apply a homogenous electric field. Samples were coated with a very thin silver electrode by screen printing. Then, the samples were co-fired at 600^{o}C for 30 min.

In order to prepare the composite for electrical measurement, fabricated piezocomposites were sliced very carefully with a certain thicknesses. Then parallel surfaces were obtained for electrical measurements.

Afterward, surfaces of piezocomposites were cleaned. Then, the piezocomposite samples were coated with a very thin silver electrode by screen printing.

All the samples were poled. Bulk samples were poled in silicon oil bath at 50^{o}C for 30 min up to 30kV and prepared 1-3 piezocomposites were poled in silicon oil bath a 50^{o}C for 30 min up to 20 kV. (Julabo Innovative Technology). Applied electric field was supplied from high voltage amplifier/controller device (Trek 610 D COR-A-TROL, USA).

Dielectric measurements of bulk samples was made with LCR meter(inductance-capacitance-resistance) (Hioki 5250-Japan) from 1kHz to 1MHz and at room temperature. Capacitance(C) and dielectric loss(D) determined and dielectric constant(K) were calculated. Curie Temperature(T_c), dielectric constant and dielectric dissipation measured with temperature dependence at 1 kHz, 10 kHz, 100 kHz and 1 MHz frequencies respectively.

Ferroelectric tester (Radiant-Precision, USA) device was used for ferroelectric measurements of bulk samples. Polarization-electric field(P-E), remanent

polarization(P_r) and coercive electric field(E_c) of the bulk samples were measured. 5-30 kV/cm range were applied to the samples.

Bipolar Strain%-Electric field was measured with the range of 5-30 kV/cm. (MTI 2000).

After poling the bulk samples, their piezoelectric constants(d_{33}) were measured with d_{33} meter (Sinocera Piezo Test Berlincourt). Measurements were taken from both directions and their average were taken to determine piezoelectric charge coefficient (d_{33}).

Measurements of 1-3 piezocomposites were made with Hioki-Japan model LCR meter(inductance-capacitance-resistance) at 1kHz and at room temperature. Capacitance(C) and dielectric loss(D) were determined and dielectric constant(K) was calculated. Curie Temperature(T_c), dielectric constant and dielectric dissipation were measured with temperature dependence at 1 kHz, 10 kHz, 100 kHz and 1 MHz frequencies respectively.

After poling the 1-3 piezocomposites, their piezoelectric constants(d_{33}) was measured with Pennebaker 8000 Piezo Test Berlincourt d_{33} meter. Measurements were taken from both directions and their average were taken to determine piezoelectric charge coefficient (d_{33}).

3.5. Preparation of Bulk Samples for IEEE Standards Measurement

Samples were prepared by columbite precursor route. Samples were prepared with ~28 mm diameter and 1 mm thickness as shown in Figure 3.2. Before sintering process, binder burned out process was carried out.

Disc samples were cut and then polarized with electric field in order to measure electromechanical properties according to IEEE Standards of piezoelectricity.

ATILA (Finite Elements Analysis) software were also used in order to proof of electromechanical properties of PNN-PZT.

3.6. Hollow Spherical Transducer Fabrication

PNN-PZT ceramic slurry were prepared to make hollow hemispherical by slip casting method. Ceramic slurry was put into hemispherical shaped plaster of paris. When plaster of paris was sucked the liquid of the slurry green ceramic had its thickness. Then hemispherical spheres were sintered, electroded and assembled to make a hollow spherical transducer. Lastly this transducer were coated with polyurethane. Flow chart fort his process is given in Figure 3.5.

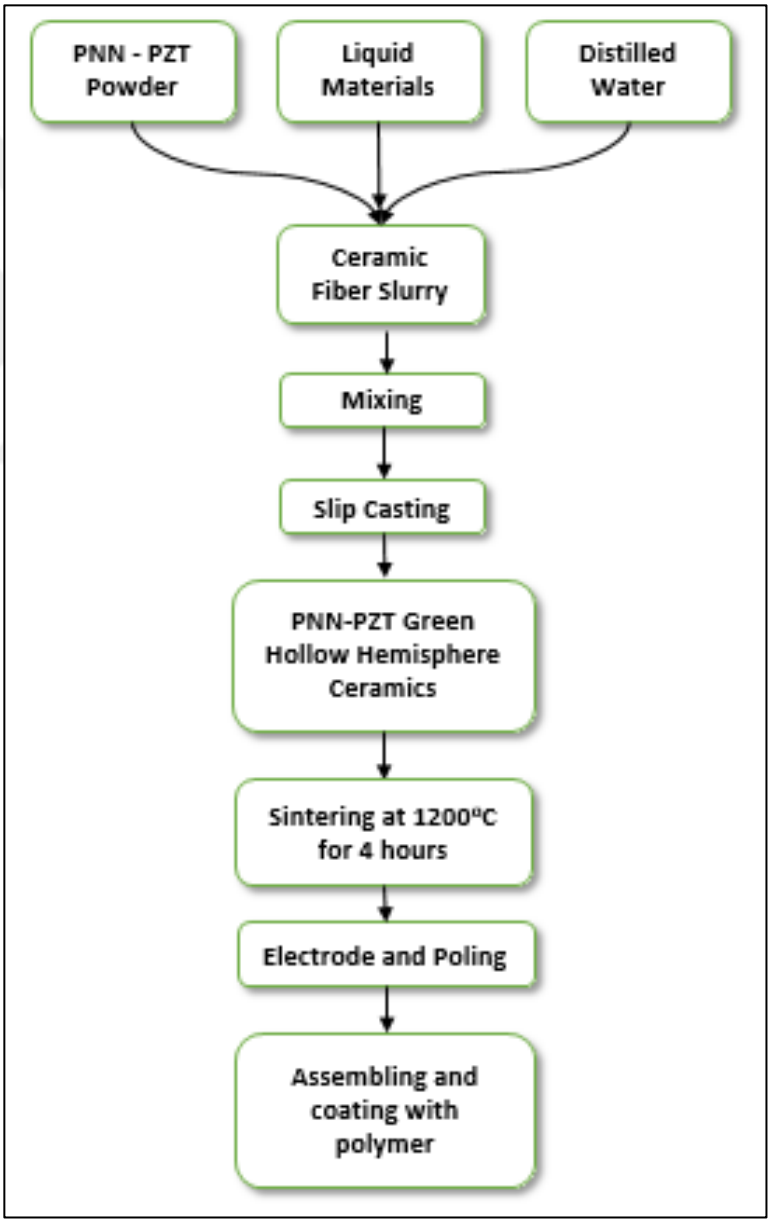

Figure 3.5: Fabrication flow chart of hollow spherical transducer.

4. RESULTS AND DISCUSSION

Results which were obtained from experimental measurements and analyses are given in this section.

4.1. Phase Analysis of PNN-PZT Compositions

4.1.1. XRD Results of Calcined PNN-PZT Powders

Lead nickel niobate zirconate titanate (PNN-PZT) powders were obtained through both mixed oxide and columbite precursor synthesizing methods. Calcination process was carried out at 1000^{o}C for 4 hours. Excess PbO was added into powders in order to compensate the Lead loss at elevated temperatures during calcination. Results of XRD analysis for the powders after calcination process is given in Figure 4.1. After calcination process, it is clearly seen that secondary phases were obtained in the samples produced by mixed oxide route. However, for the columbite precursor method; secondary phases were not obtained after calcination. This difference may be due to the presence of Niobium in the composition. As Niobium(Nb) is such a pyrochlore former, it is difficult to obtain pure perovskite phase by mixed oxide fabrication method with the compositions containing Niobium. [J. Chen, M. P. Harmer, 1990] [M. Dambekalne et al., 1989].

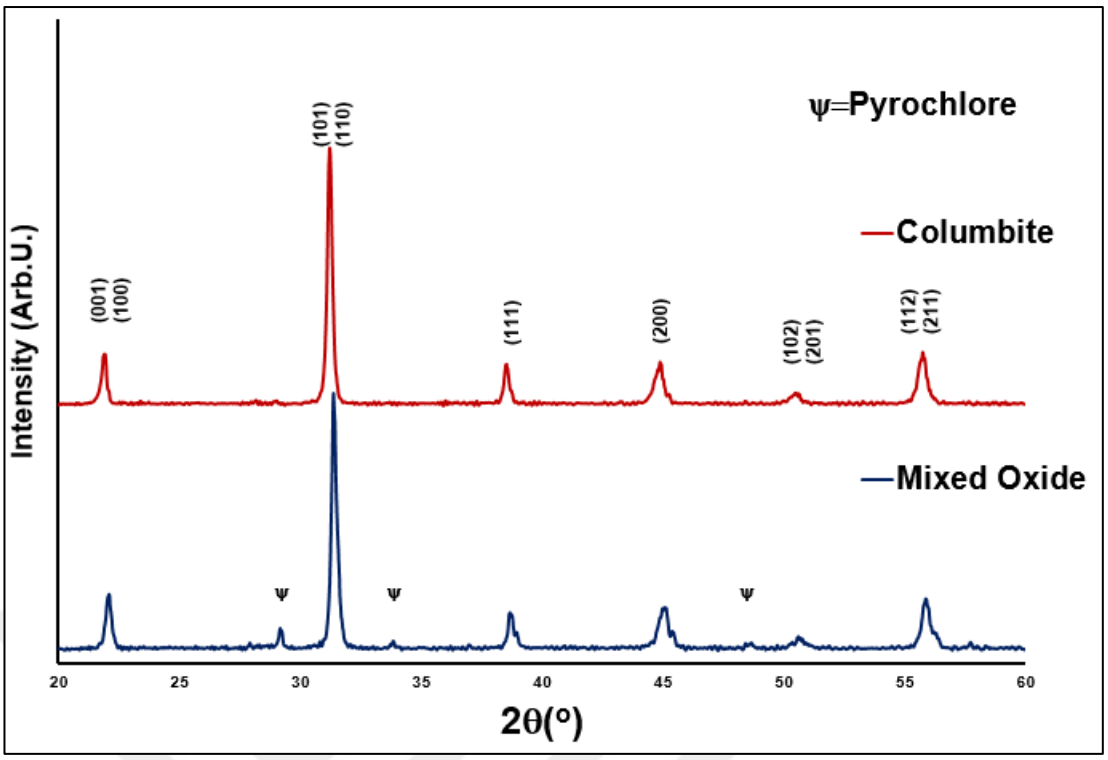

Figure 4.1: XRD patterns of calcined powders of PNN-PZT composition prepared by mixed oxide route and columbite route.

In order to prevent pyrochlore formation in the composition, it is seen that more pure perovskite can be achieved by columbite route even after calcination process [Bove et al, 2001].

4.1.2. XRD Results of Sintered PNN-PZT Bulk Samples

Sintering process was carried out at 1200^{o}C for 4 hours. Excess PbO was added into calcined powders in order to compensate the Lead loss at elevated temperatures during sintering process. As it is seen in Fig. 4.2, after sintering, secondary phases which were existed after calcination were vanished for the bulk sample which were prepared by mixed oxide route. There was already no secondary phases after calcination for the bulk samples which were prepared by columbite precursor route.

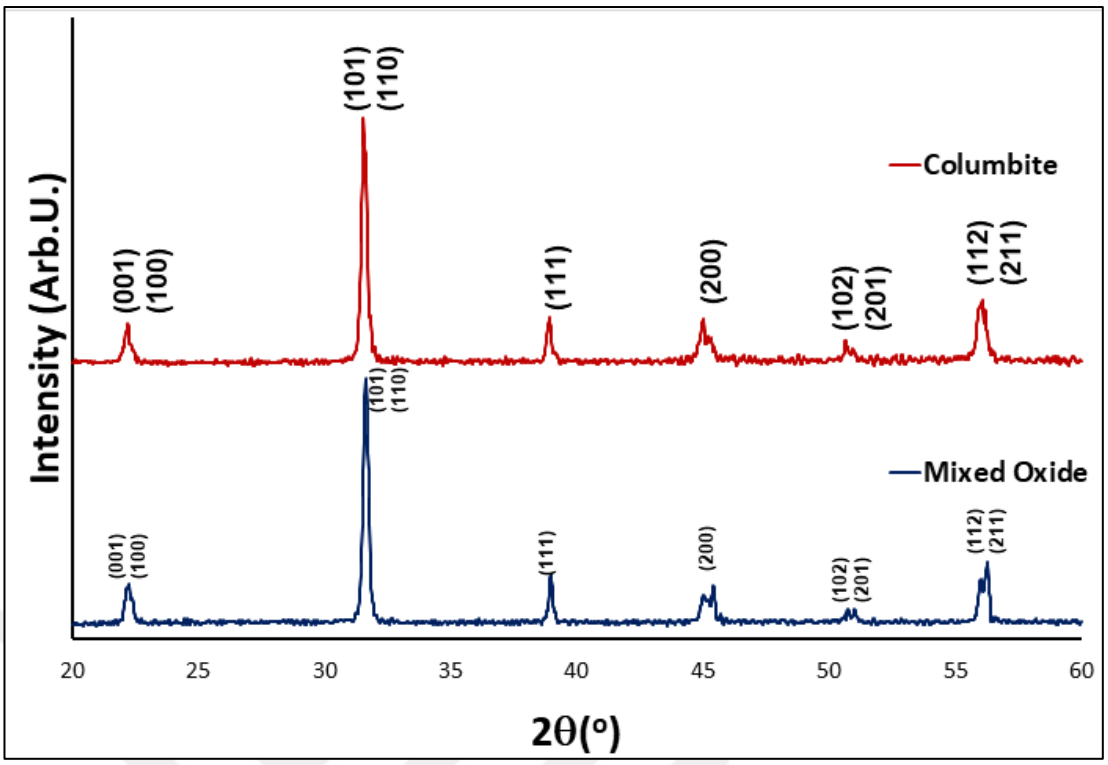

Figure 4.2: XRD pattern of sintered bulk samples of PNN-PZT using different powders.

4.1.3. Microstructural Analyses of The Sintered Bulk and Fiber PNN-PZT Samples

SEM images of the sintered bulk samples prepared by both mixed oxide and columbite precursor route were given in Figure 4.3 and Figure 4.4. By looking these images, it is clear to seen that the pore percentage is low in the structure for both fabrication route. Densities of the samples were measured by Archimedes' principle. The results of the densities were 8,0 and 8,1 gr/mm^2 for Mixed oxide route and Columbite precursor route respectively. SEM images shows that there is no big structural difference between the structures of samples fabricated from the powders using mixed oxide and columbite route.

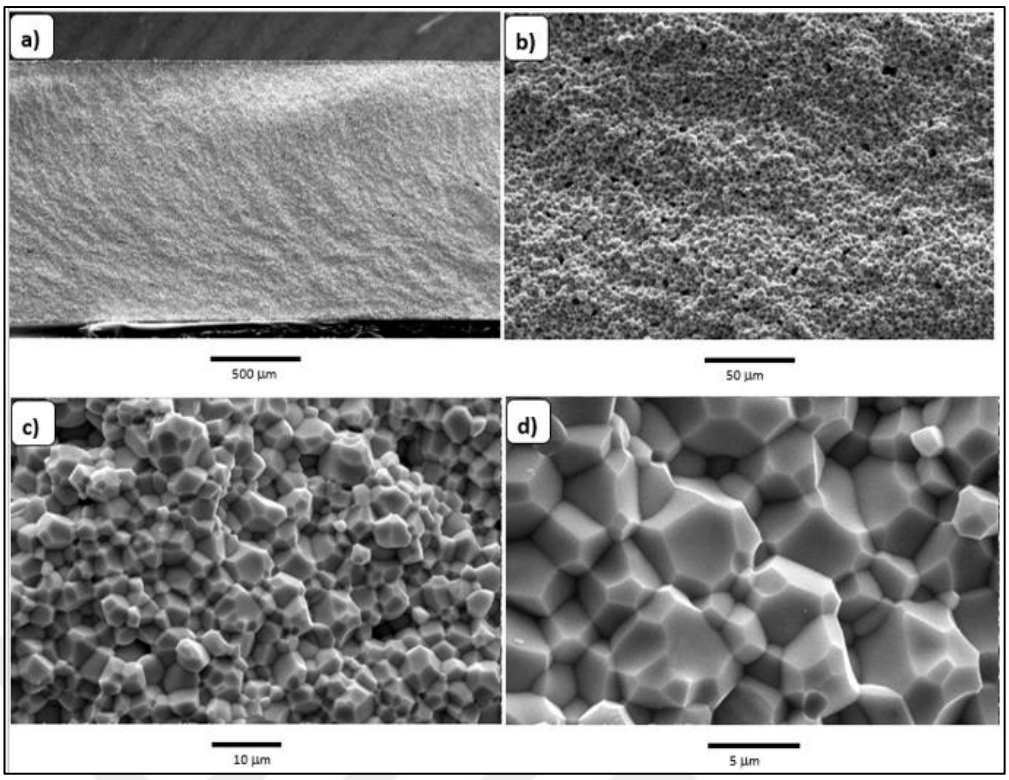

Figure 4.3: SEM micrographs for the bulk samples sintered at 1200ºC for 4 hours using powders fabricated by mixed oxide route. a) 50x b) 500x c) 2000x d) 5000x

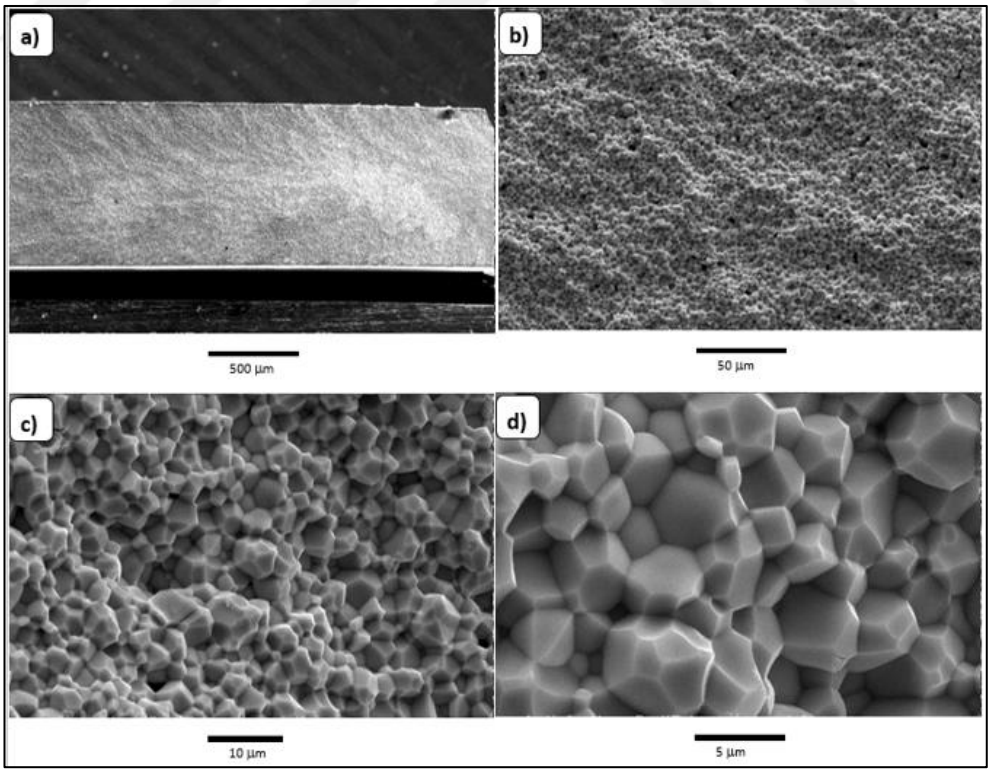

Figure 4.4: SEM micrographs for the bulk samples sintered at 1200ºC for 4 hours using powders fabricated by columbite route. a) 50x b) 500x c) 2000x d) 5000x

Figure 4.3 and Figure 4.4 shows that the structure is dense and without porosity.

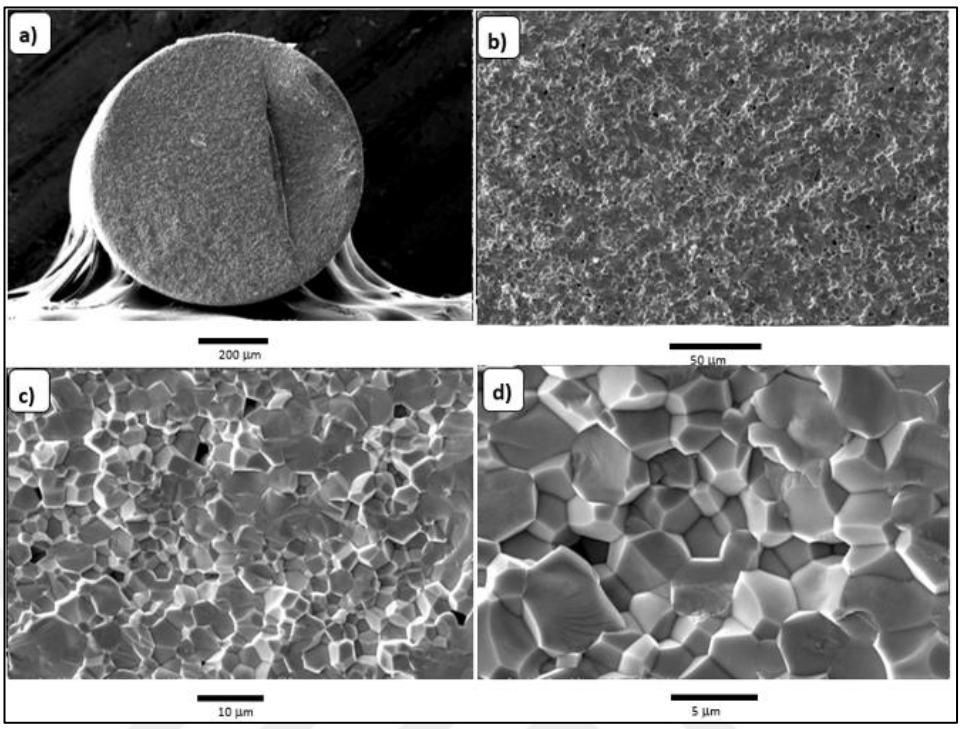

Figure 4.5: SEM micrographs of fiber fracture surface fabricated by columbite route. a) 100x b) 500x c) 2000x d) 5000x

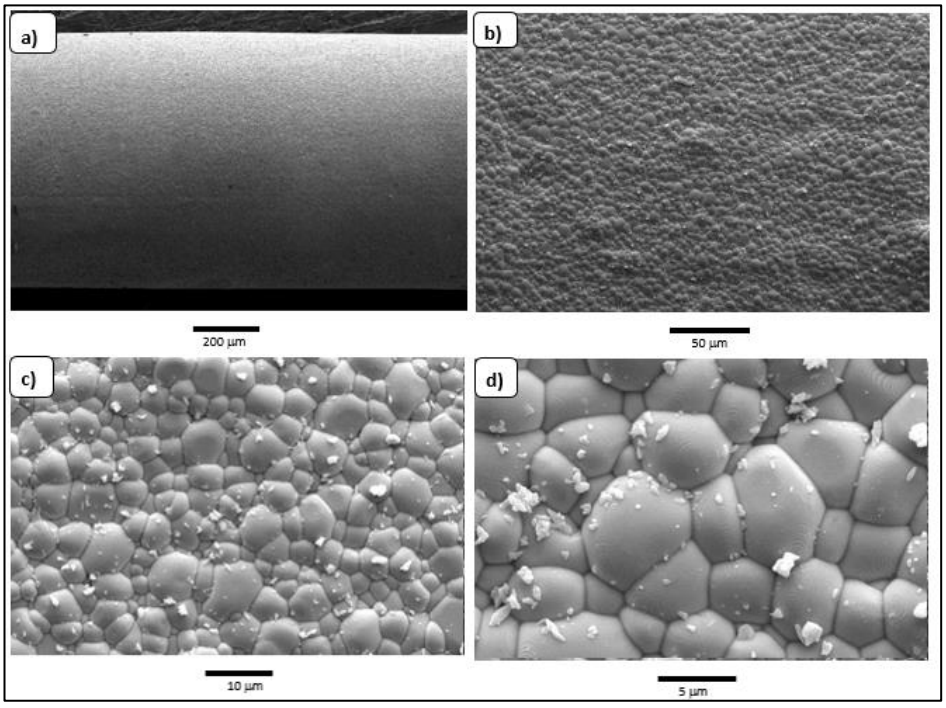

Figure 4.6: SEM micrographs of fiber surface fabricated by columbite route. a) 100x b) 500x c) 2000x d) 5000x

4.2. Polarization and Strain Behaviour of PNN-PZT Bulk Samples

Polarization-electric field results of bulk samples will be discussed in this section. Hysteresis loops for the samples fabricated with both mixed oxide route and columbite route are given in Figure 4.7. Samples have same surface areas and thicknesses. Electric field was applied to the samples up to 30 kV and remnant polarizations were measured. In these samples fabricated by mixed oxide method average values were $2P_r$=56,266 μC/cm^2, $2E_c$=11,583 kV/cm.

In these samples fabricated by columbite method average values were $2P_r$=59,178 μC/cm^2, $2E_c$=11,698 kV/cm. There is slight increase of remnant polarization of the samples fabricated by columbite route. This may be due to having more pure perovskite phase can be achieved by columbite route than mixed oxide route since Niobium is such a pyrochlore former [Chen and Harmer, 1990].

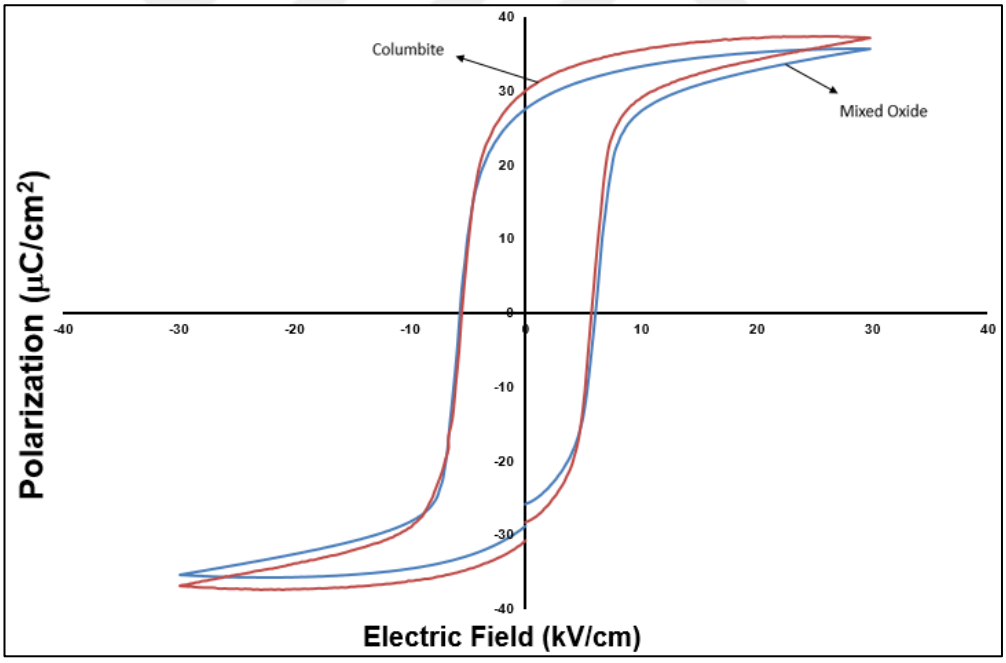

Figure 4.7: Polarization-electric field hysteresis loops of bulk samples fabricated by both mixed oxide and columbite routes.

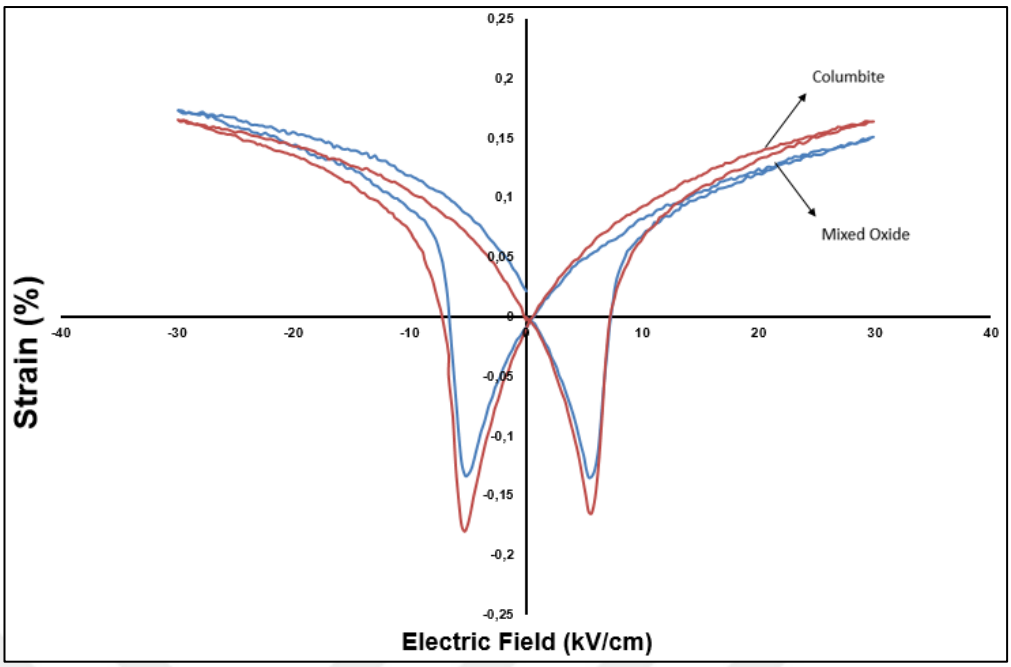

Figure 4.8: Strain-Electric field curve of bulk samples fabricated by mixed oxide route.

Strain-electric field values were also measured for the same samples. The measurement was made up to 30 kV. As it is seen in Figure 4.8 strain values against electric field are very similar, however, samples which were fabricated with columbite route have more strain value than samples fabricated mixed oxide route. This difference may be due to the pyrochlore free perovskite formation in columbite route [Chen and Harmer, 1990].

Polarization-electric field and strain-electric field graphs of bulk samples which were sintered at 1100^{o}C, 1150^{o}C, 1200^{o}C and 1250^{o}C were also given in Figure 4.9 and Figure 4.10 comparatively.

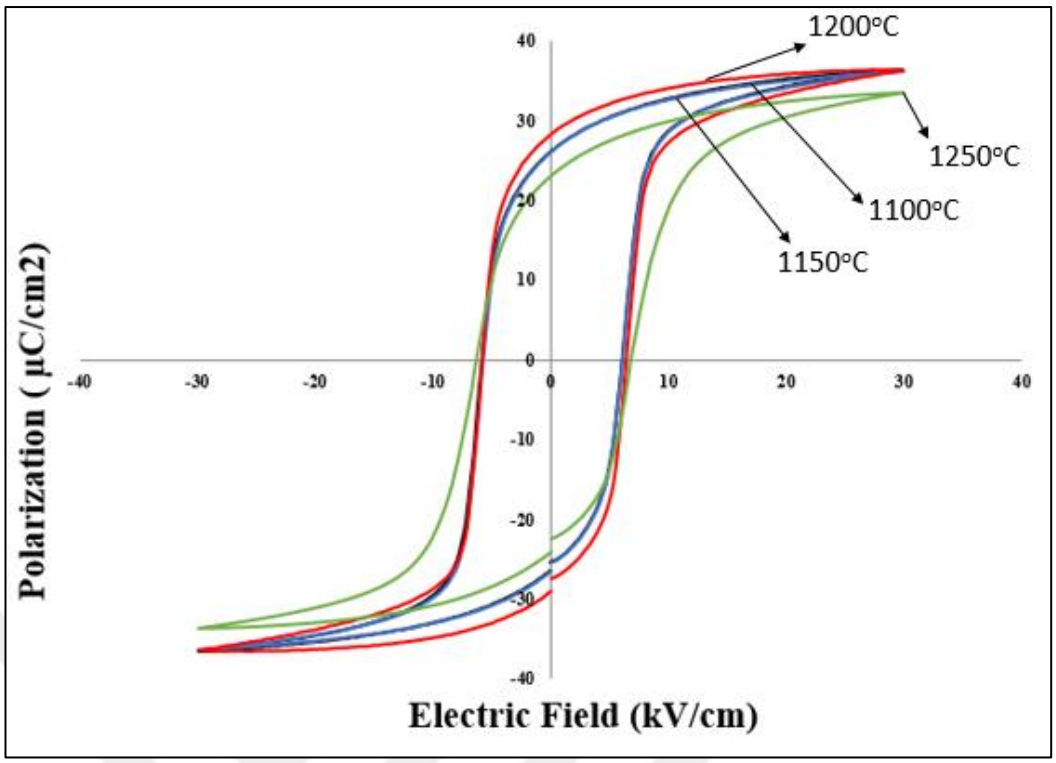

Figure 4.9: Polarization-electric field hysteresis loops of bulk samples sintered at different temperatures

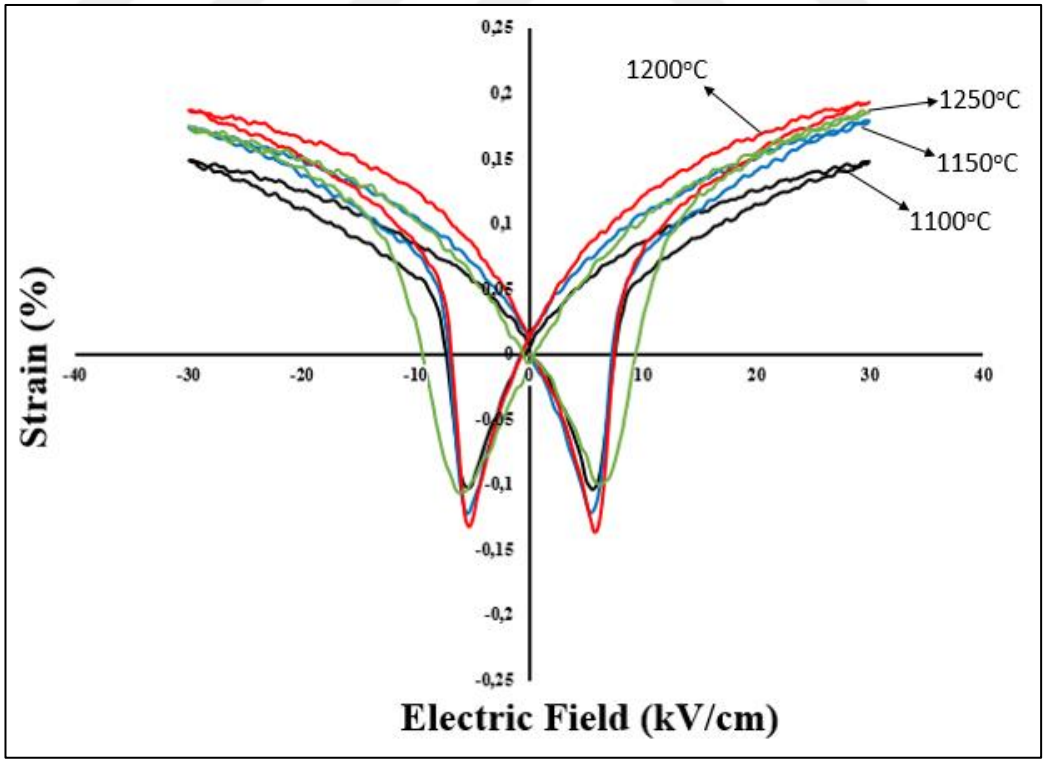

Figure 4.10: Strain-electric field curves of bulk samples sintered at different temperatures.

4.3. Electromechanical Properties of PNN-PZT Bulk Samples

In this section electromechanical properties of bulk samples were given for both mixed oxide route and columbite route comparably. It is clearly seen in Table 4.2 that there is an increase of electrical properties when it is fabricated by columbite route.

Table 4.1: Comparison of electromechanical properties of the samples fabricated by mixed oxide and columbite route comparably.

Sample	k_p	k_t	ε_{33}^T	d_{33}
Mixed Oxide	0.61	0.51	5052	630
Columbite	0.67	0.53	5910	820

Table 4.2 shows that higher dielectric constant, higher electromechanical coupling factor can be achieved by columbite route.

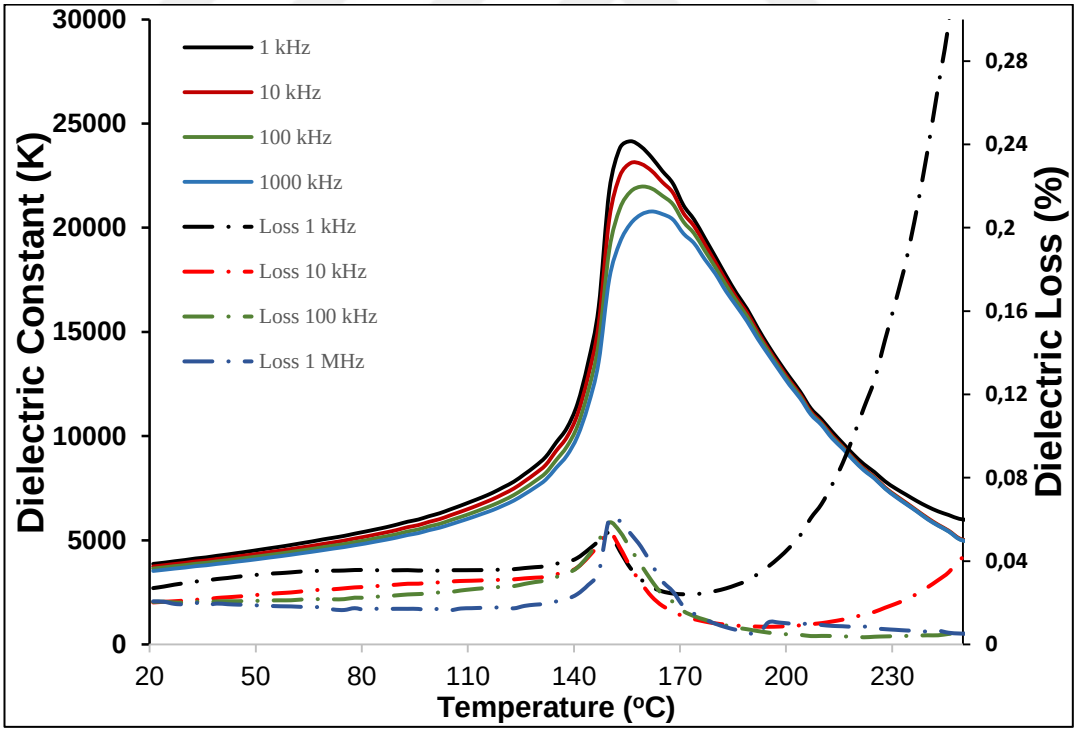

Figure 4.11: Dielectric constant(K) and dielectric loss(tanδ) versus temperature for the sample fabricated by mixed oxide route.

Figure 4.11 and Figure 4.12 show that columbite route gives higher dielectric constant(Table 4.3) than mixed oxide route although there is no big difference of dielectric loss for both fabrication method.

Dielectric constants(K) of the samples fabricated by mixed oxide route were measured at different frequencies and different temperatures. Dielectric constants at room temperature were 4050, 3915, 3807 and 3688 at frequencies 1 kHz, 10 kHz, 100 kHz and 1 MHz respectively. As it can be seen in Fig. 4.11 these constants reach their maximum levels as 24153, 23103, 21730 and 20189 at frequencies 1 kHz, 10 kHz, 100 kHz and 1 MHz respectively.

Dielectric losses(tanδ) of the samples fabricated by mixed oxide route were also measured at different temperatures at different frequencies. Dielectric losses at room temperature are 2.9%, 2.1%, 2.0% and 1.9% at frequencies 1 kHz, 10 kHz, 100 kHz and 1 MHz respectively. As it can be seen in Figure 4.11 these losses reach 3.6%, 3.7%, 4.6% and 5.3% at frequencies 1 kHz, 10 kHz, 100 kHz and 1 MHz respectively.

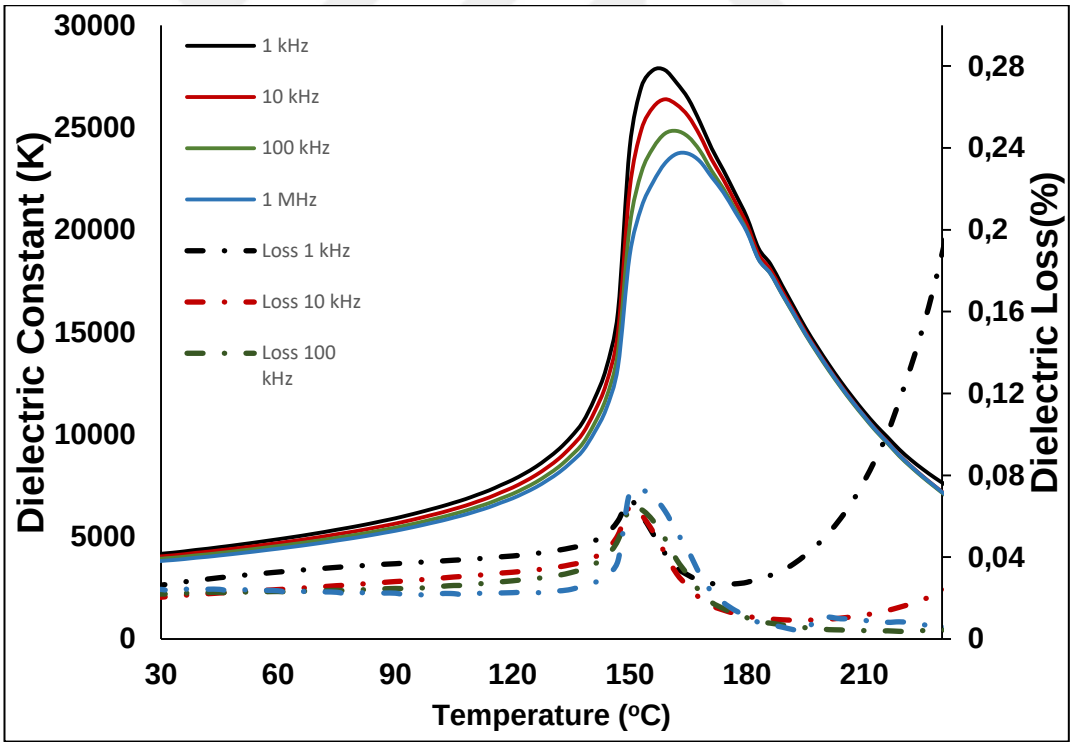

Figure 4.12: Dielectric constant(K) and dielectric loss(tanδ) values versus temperature for the sample fabricated by columbite route.

Dielectric constants(K) of the samples fabricated by columbite route were measured at different frequencies and different temperatures. Dielectric constants at

room temperature are 4162, 4035, 3923 and 3811 at frequencies 1 kHz, 10 kHz, 100 kHz and 1 MHz respectively. As it can be seen in Figure 4.12 these constants reach 27810, 26377, 24698 and 23240 at frequencies 1 kHz, 10 kHz, 100 kHz and 1 MHz respectively.

Dielectric losses(tanδ) of the samples fabricated by columbite route were measured at different temperatures at different frequencies. Dielectric losses at room temperature are 2.6%, 2.0%, 2.1%, and 2.4% at frequencies 1 kHz, 10 kHz, 100 kHz and 1 MHz respectively. As it can be seen in Figure 4.12 these constants reach 4.1%, 4.2%, 4.9% and 6.3% at frequencies 1 kHz, 10 kHz, 100 kHz and 1 MHz respectively.

As it is seen in Figure 4.11 and Figure 4.12 there is no certain Tc, instead, there is a diffuse phase transition. And Curie temperature increases with the increased frequency while dielectric constant decreases (Fig. 4.11 and Fig. 4.12). This shows that this composition has relaxor ferroelectric property [Uchino, 2000].

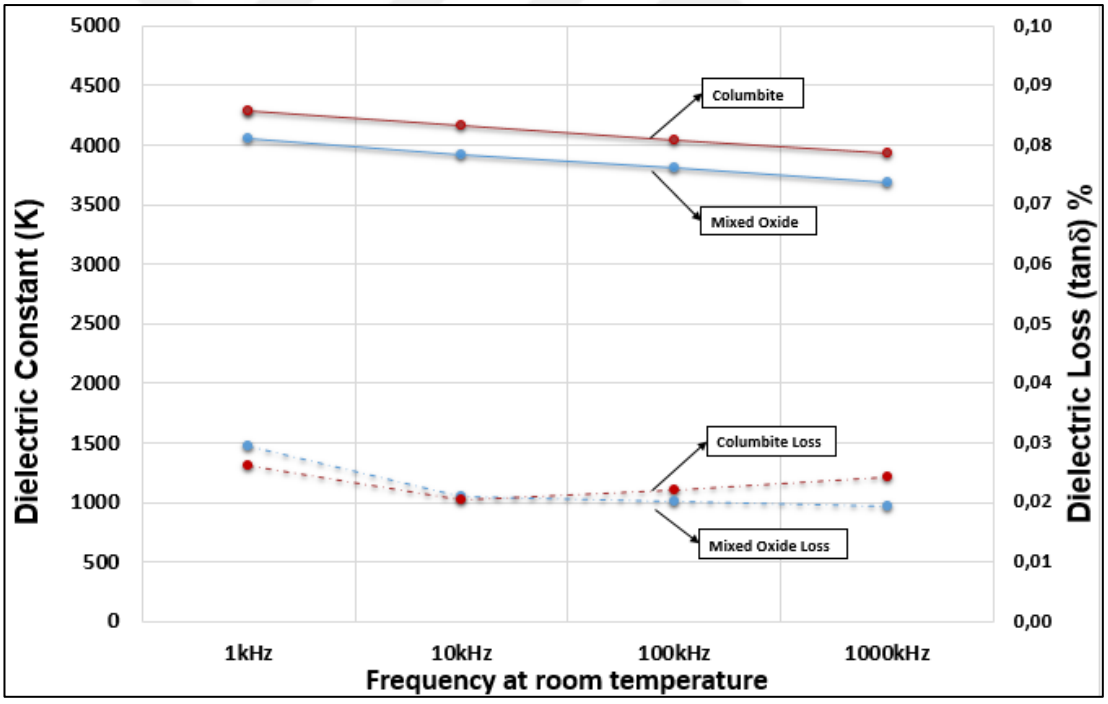

Figure 4.13: Dielectric constant(K) and dielectric loss(tanδ) values at room temperature at different frequencies for Mixed Oxide and Columbite route comparably

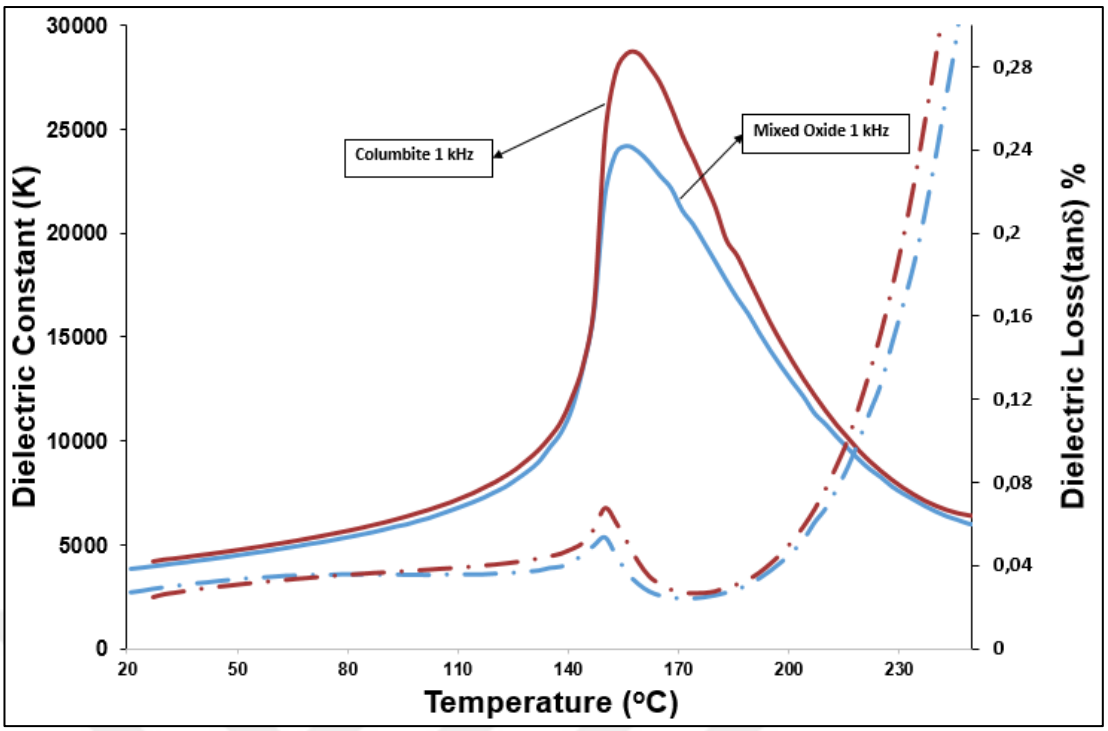

Figure 4.14: Dielectric constant(K) and dielectric loss(tanδ) at 1kHz frequency as a function of temperature for Mixed Oxide and Columbite route comparably

It is clearly seen in Figure 4.13 and Figure 4.14 that the dielectric constant gets higher when samples were prepared with columbite precursor route. These results may be because of having a better perovskite formation can be achieved with columbite route [Bove et. al. 2001].

Because of these comparisons of electromechanical properties and polarization for both fabrication methods the columbite route was chosen to step further on the study and fabricated the fiber from columbite route synthesizing.

4.4. Results for Electromechanical Properties

Electromechanical property matrixes were calculated by using resonance mode measurements from disc and plate-shaped samples according to IEEE standards of piezoelectricity. Results for these samples were given in Table 4.2. In this table, also, electromechanical properties for PZT 5H [Sunnytech] were given in order to compare with this study.

Table 4.2: Electromechanical and Dielectric Properties of PNN-PZT and Commercial PZT 5H

PROPERTIES	**PNN-PZT1**	**PNN-PZT2**	**PZT 5H**	**PNN-PZT***
Density ρ(kg/m^3)	8100	8100	7600	7800
Electromechanical Coefficients (%)				
k_p	67	67	77	60
k_t	53	50	52	47
k_{31}	39	39	42	-
k_{33}	78	77	-	-
k_{15}	59	57	-	-
Piezoelectric Charge Constants (pC/N)				
d_{31}	-337	-335	-290	-
d_{15}	631	622	-	-
d_{33}	820	820	650	640
Elastic Compliance Coefficients (x10-12)m^2/N				
S_{11}^E	14.7	14.1	14.1	-
S_{12}^E	-4.72	-4.72	-	-
S_{13}^E	-8.32	-8.39	-	-
S_{33}^E	22.5	22.9	-	-
S_{44}^E	38.2	38.3	-	-
Dielectric Constants at RT (1 kHz)				
ε_{11}^T	5161	4879	-	-
ε_{33}^T	5910	5779	3800	3800
Dielectric Loss at RT (1 kHz) (%)				
tanδ	1.8	1.7	1.7	1.7
Mechanical Quality Factor				
Q_m	85	89	65	65
Mechanical Loss (1/Q_m)				
tanμ	0.012	0.011	0.015	-

Table 4.2 shows that PNN-PZT composition attracts attention due to its superior electromechanical properties. This composition is suitable to be used in many kinds of applications with its higher properties.

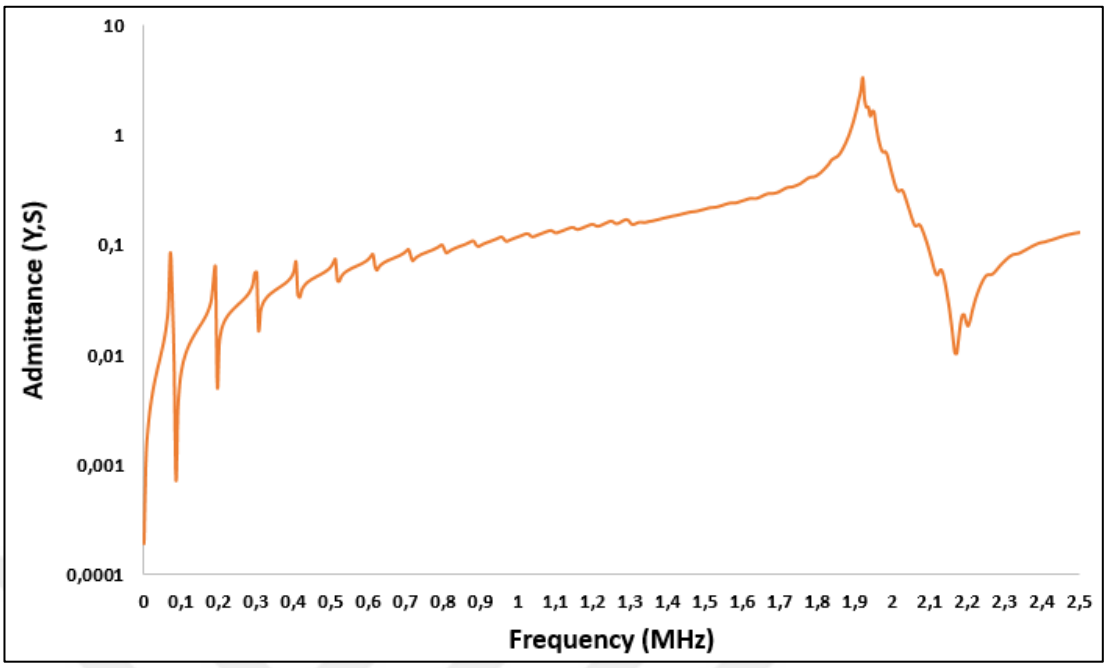

Figure 4.15: Admittance-frequency graph of experimentally measured PNN-PZT composition

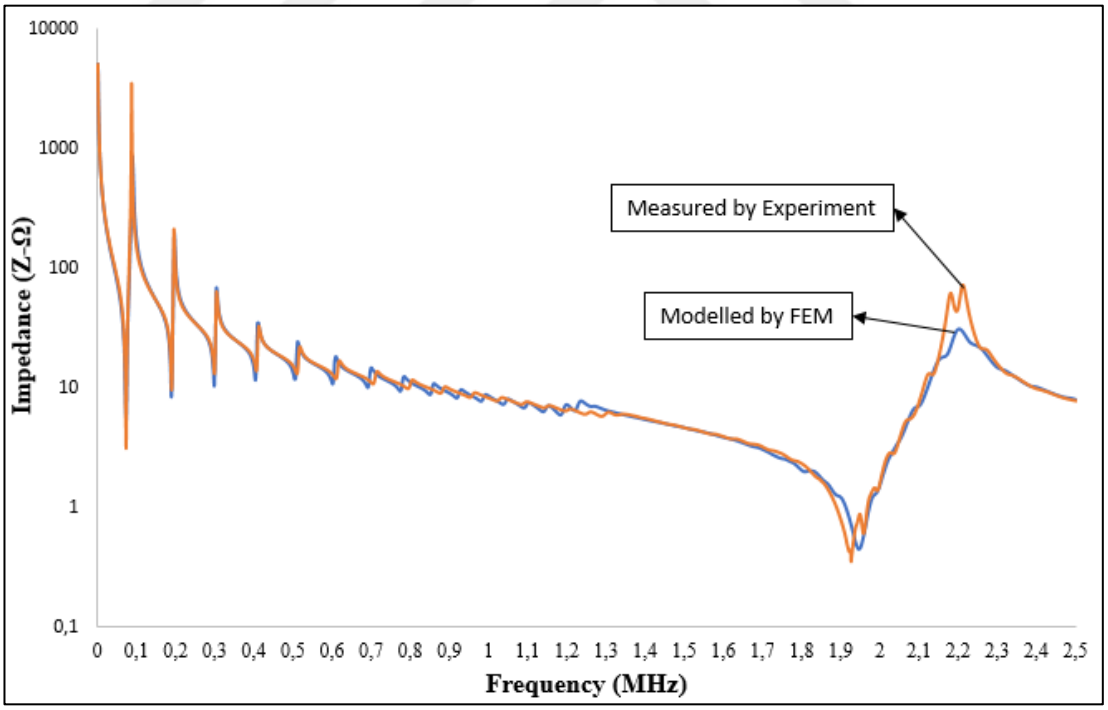

Figure 4.16: Impedance-Frequency graph of both measured and modelled PNN-PZT composition

Experimentally measured admittance-frequency graph of PNN-PZT is shown in Figure 4.15. In Figure 4.16, Finite Elements Analysis results were confirmed the calculated electromechanical properties of PNN-PZT. As a result, pre-calculations were found quite accurate.

4.5. Results For Fiber Fabrication and Piezocomposites

PNN-PZT fibers were made by alginate gelation route have ~550 μm average diameter. It is prepared as 2 mm length for making 1-3 connected piezocomposites. Piezocomposites made with hexagon shape with %10 approximate volume ratio and sliced with 1 mm length (Figure 4. 17).

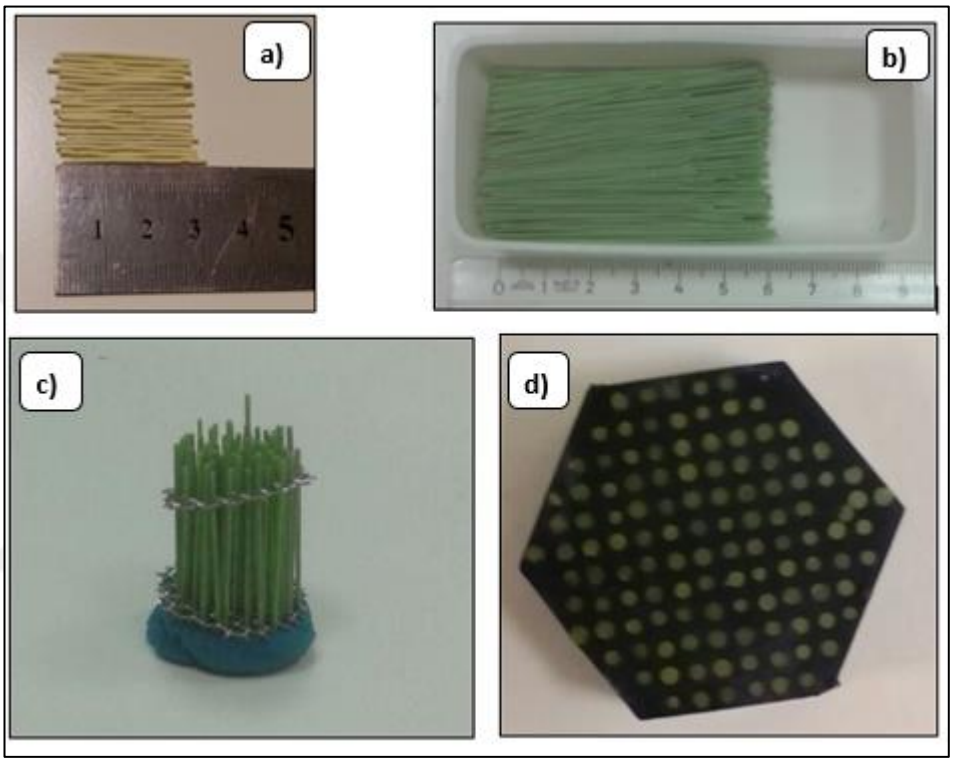

Figure 4.17: a) PNN-PZT green ceramic fibers fabricated by alginate gelation route. b) Sintered PNN-PZT ceramics c) Aligned ceramics d) Piezocomposite with 1-3 connectivity

4.6. Results of Hollow Spherical Transducer

Hollow hemispherical PNN-PZT ceramics with ~1,55 mm thicknesses and ~20,25 mm outter diameters were obtained by slip casting method. Then two hollow hemispherical ceramics were assembled together in order to have a whole hollow spherical transducer. Last step was to coat the transducer with polyurethane (Figure 4.18).

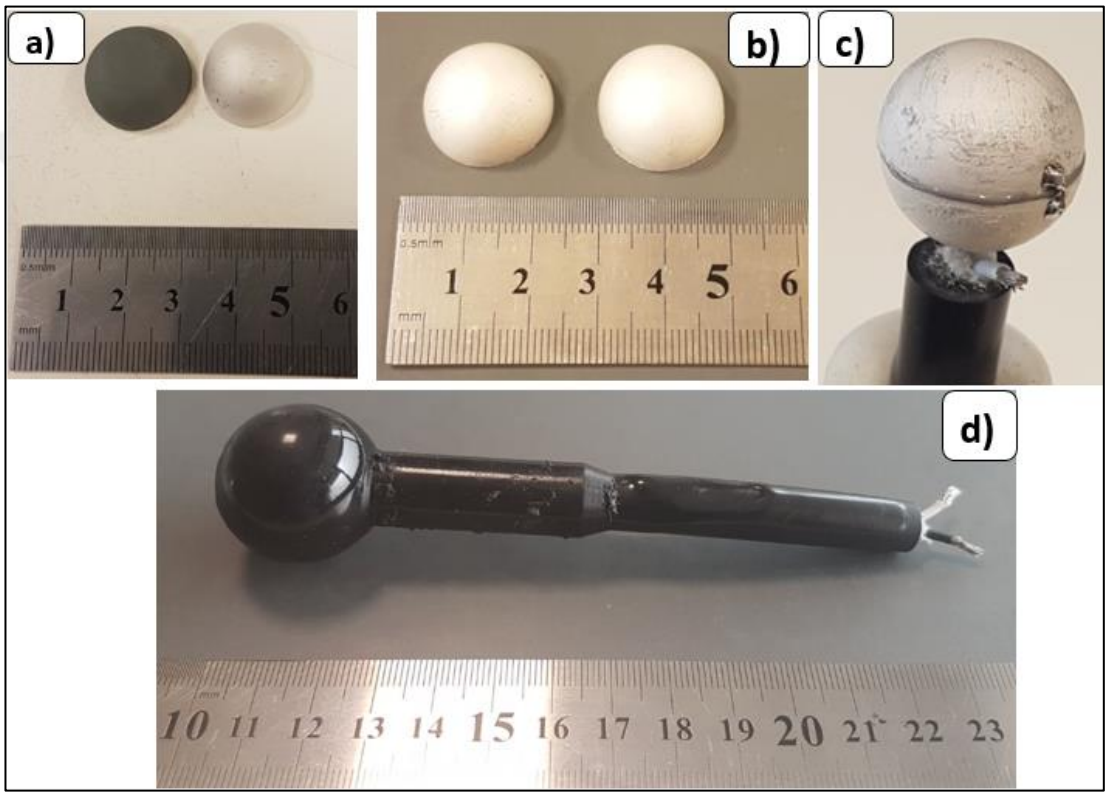

Figure 4.18: Hollow spherical transducer fabrication. a) Sintered hollow hemispherical PNN-PZT ceramics with and without electrode. b) Sintered hollow hemispherical PNN-PZT ceramics with electrode. c) Assembled hollow spherical transducer from two hemispherical ceramics. d) Polyurethane coated hollow spherical transducer

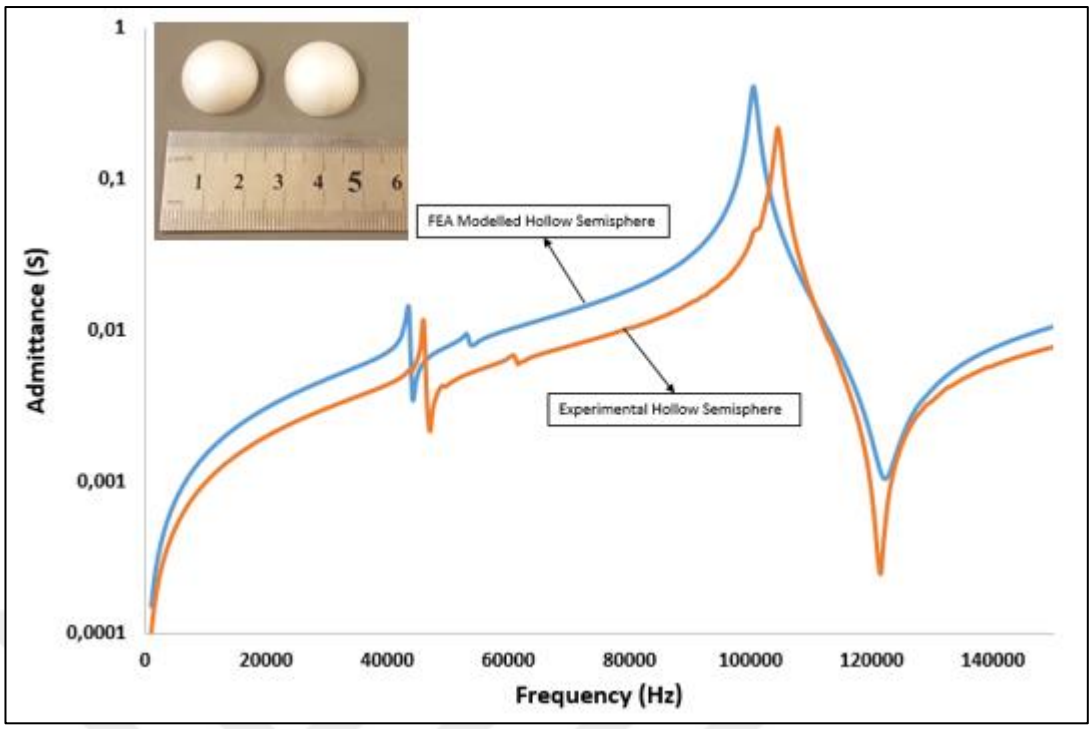

Figure 4.19: FEA modelled results vs. experimental results of hollow hemispherical PNN-PZT ceramics.

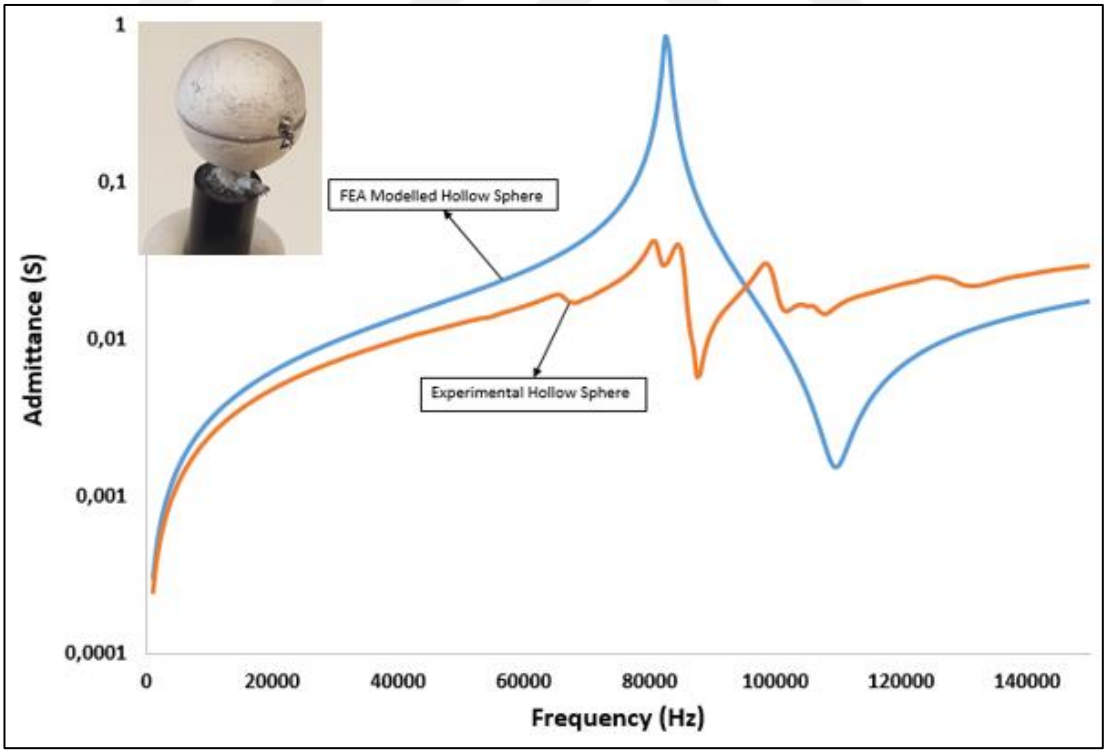

Figure 4.20: FEA modelled results vs. experimental results of hollow spherical transducer.

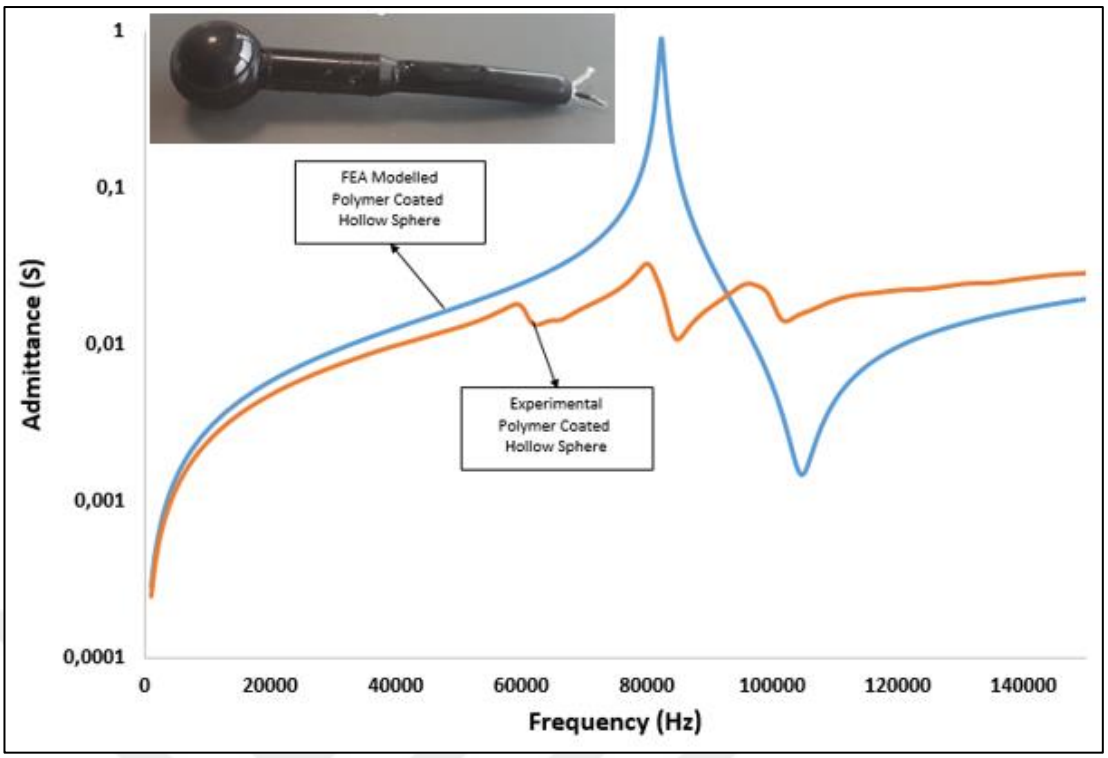

Figure 4.21: FEA modelled results vs. experimental results of hollow spherical transducer coated with polyurethane.

Figure 4.19, Figure 4.20 and Figure 4.21 shows finite element analysis results against experimental result for hollow hemispherical PNN-PZT ceramics, hollow spherical transducer and hollow spherical transducer with polyurethane coated respectively. These results shows that PNN-PZT ceramics are capable for some underwater, medical etc. applications.

5. CONCLUSION

One of the problems of complex relaxor ferroelectrics containing Niobate(Nb_2O_5) such as PMN, PZN, PNN etc. is that having single perovskite phase is difficult since Niobium(Nb) is such an effective pyrochlore former. When it is prepared in conventional mixed oxide route, during calcination PbO and Nb_2O_5 forms as a pyrochlore phase at earlier stages in calcination. Therefore, it is difficult to have pure perovskite phase with the compositions containing of niobium than lead zirconate titanate(PZT). Pyrochlore phase has a low dielectric constant (~200) and commonly believed that this decreases electromechanical properties of the composition [J. Chen and M. P. Harmer, 1990] [M. Dambekalne et al. 1989][Damjanovic, 2001][Swartz and Shrout, 1982]. For these reason proper processing should be done to overcome this problem and reproducibility in these complex relaxor ferroelectrics. In order to have a better perovskite phase with normal-relaxor PNN-PZT composition, another fabrication method called as "columbite precursor method" was investigated in this study. First bulk samples was prepared and fabricated by both mixed oxide and columbite precursor route comparably. Obtained electromechanical properties such as Pr, Er, d_{33}, k_{eff}, K were superior in columbite route than mixed oxide route. Therefore fabrication route for powder was columbite route in fiber and hollow sphere fabrication.

Also, fiber drawing by alginate gelation [Alkoy, 2007] route was also investigated in this study. Finally, dense PNN-PZT fibers with 550 μm approximate diameters were obtained. These ceramic fibers with high electromechanical properties can be used in some underwater and medical applications. One of the limitation in piezoelectric ceramics is that their figure of merit in underwater acoustic applications. In order to overcome this limitation and develop its efficiency in these application there are some different designs in the literature called as "piezoelectric composites" [Newnham et. al. 1999]

In this study 1-3 piezocomposites and their producibility were also investigated. With the PNN-PZT fibers drawn by alginate gelation route are fabricated as 1-3 connected piezocomposites.

Electromechanical properties of the samples modelled by FEM(ATILA) and experimentally measured according to IEEE standards in order to remark its superior properties againts to commercial PZT5H and commercial PNN-PZT.

Also hollow sphere transducer were successfully made by this composition. First semi hollow sphere was made by slip casting. Then two pieces of semi hollow spheres were mounted after sintering and electroding. Modelling by FEM and measured electrical properties shown that it is suitable for underwater applications.

With its superior electromechanical properties and producibility of fibers from PNN-PZT composition it is expected to be highly utilized in underwater passive sensor, medical applications and many more. As it is difficult to produce PNN-PZT composition and its processing is still a challenge, it can be improved to have superior characteristic of it by changing the composition ratios and fabricating the composition with different methods.

B-site precursor production method of PNN-PZT may increase the electrical properties of the composition.

As PNN-PZT has relatively superior electrical properties than commercial examples, different compositions and dopants may be beneficial for some certain commercial applications.

REFERENCES

Akça E., (2010), "Kurşun esaslı elektroseramik tozların sentezlenmesi ve seramiklerin üretilmesi ve karakterizasyonları", Yüksek Lisans Tezi, Gebze Yüksek Teknoloji Enstitüsü.

Alkoy S., Tressler J.F., Doğan A., Newnham R.E., (1999), "Functional composites for sensors, actuators and transducers", Elsevier.

Alkoy S., Yanık H., Yapar B., (2007) "Fabrication of Lead Zirconate Titanate Ceramic Fibers by Gelation of Sodium Alginate", Ceramics International 33, 389–394.

B . Jaffe, R. S. Roth, S. Marzull, (1954), 'Piezoelectric properties of lead zirconate-lead titanate solid solution ceramics', J. Appl. Phys. 25, 809–810.

B. Jaffe, W. R. Cook, H. Jaffe, (1971), "Piezoelectric Ceramics, New York: Academic Press", 142.

C. A. Randall, A. S. Bhalla, (1990), " Nanostructural-Property Relations in Complex Lead Perovskites" Jpn. J. Appl. Phys., Part 1 29, 327.

Carter C.B., Norton M.G., (2007), "Ceramic Materials- Science and Engineering", 0-387-46271-6, Springer.

Draget K. I., Semidsrød O., Skjåk-Bræk G., (2005), "Alginates From Algea", Willey-VCH, Verlag GmbH & Co. KGaA, Weinheim.

E. F. Alberta, A. S. Bhalla, (2001), ''Piezoelectric and Dielectric Properties of Transparent $Pb(Ni_{1/3}Nb_{2/3})_{1-x-y}Zr_xTi_yO_3$ Ceramics Prepared by Hot Isostatic Pressing'' Inorganic Materials.

Gururaja T. R. (1994), "Piezoelectrics for Medical Ultrasonic Imaging" American Ceramic Society Bulletin 73, 50-55.

Haertling G. H., (1999), "Ferroelectric Ceramics: History and Technology", J. Am. Ceram. Soc., 82(4), 797- 818.

J. Chen, M. P. Harmer, (1990), "Microstructure and Dielectric Properties of Lead Magnesium Niobate-Pyrochlore Diphasic Mixtures," J. Am. Ceram. Soc., 73, 68–73

J. F. Tressler, S. Alkoy, R. E. Newnham, (1998), "Piezoelectric Sensors and Sensor Materials" J. Electroceram. 2, 257–272.

Janas V. F.
Safari A., (1995), "Overview of Fine-Scale Piezoelectric Ceramic/Polymer Composite Processing'', J. American Ceramic Society, 78, 2945-2955.

Jia Y., Kano Y., Zhi-peng Xie, (2002), "New gel-casting process for alumina ceramics based on gelation of alginate", Journal of European Ceramic Society 22, 1911–1916.

Jordan T.L., Quanies Z., (2001), “Piezoelectric Ceramics Characterization”, NASA/CR-2001-211225, ICASE Report No. 2001-28.

Kao K.C., (2004), “Dielectric Phenomena in Solids: With Emphasis on Physical Concepts of Electronic Processes”, Elsevier, Inc.

Klicker K.A., Biggers J.V., Newnham R.E., (1979), “Composites of PZT and epoxy for hydrostatic transducer applications”, Electronic Division Fall Meeting, The American Ceramic Soc. Williamsburg, Virginia.

L. E. Cross, (1987), “Relaxor Ferroelectrics,” Ferroelectrics, 76, 241–67.

M. Dambekalne, I. Brante, A. Sternberg, (1989), “The Formation Process of Complex Lead-Containing Niobates,” Ferroelectrics, 90, 1–14.

Matthias B T and Remeika J P , (1949), ‘Ferroelectricity in the ilmenite structure’, Phys Rev, 76, 1886–1887.

Newnham R.E., (2005) “Properties of Materials- Anisotropy, Symmetry and Structure”, 0-19-852075-1, Oxford University Press.

Newnham R.E., (2004), “Fifty Years of Ferroelectrics”, IEEE International Ultrasonics, Ferroelectrics and Frequency Control Joint 50th Anniversary Conference, Montreal, Canada, 1-6.

Newnham R.E., Fernandez J.F., Markowski K.A., Fielding J.T., Dogan A., Wallis J., (1994), “Composite piezoelectric sensors and actuators”, Symposium I1, MRS Fall Meeting.

R. E. Newnham R. E., D.P. Skinner, L.E. Cross, (1978), “Connectivity and piezoelectric-pyroelectric composites”, Mat. Res. Bull., vol. 13(5), 525- 536.

Newnham R.E., Ruschau G.R., (1991), “Smart Electroceramics” J Am Ceram Soc ,74 131 463-80.

Robert G., Damjanovic D., Demartin M. (1998), ” Phase Diagram for the $0.4Pb(Ni_{1/3},Nb_{1/3})O_3–0.6Pb(Zr,Ti)O_3$ Solid Solution in the Vicinity of a Morphotropic Phase Boundary” J. Am. Ceram. Soc.

Robert G., Damjanovic D., Demartin M., Nava Setter (2001), ” Synthesis of Lead Nickel Niobate–Lead Zirconate Titanate Solid Solutions by a B-site Precursor Method” J. Am. Ceram. Soc., 84 (12) 2869–72.

S. L. Swartz, T. R. Shrout, (1982), “Fabrication of Perovskite Lead Magnesium Niobate,” Mafer. Res. Bull., 17, 1245-50.

Skinner D.P., Newnham D.P., L.E. Cross, (1978), “Flexible composite transducers”, Mater. Res. Bull. 13(6), 599–607.

Smith W.A., (1992), “New opportunities in ultrasonic transducers emerging from innovations in piezoelectric materials”, Invited Paper, SPIE Vol. 1733, 1-26.

Smith, WF, (1990), "Principles of Materials Science and Engineering", 2nd Edn., McGraw-Hill.

T. Bove, W. Wolny, E. Ringgaard, A. Pedersen, (2001), “New piezoceramic PZT-PNN material for medical diagnostics applications”, J. Eur. Ceram. Soc. 21.

Uchino K., (2000), “ Ferroelectric Devices”, 0-8247-8133-3, Marcel Dekker, Inc.

Uchino K., (2010), “Advanced Piezoelectric Materials” 978-1-84569-534-7, Wood Head Limited Co.

V. A. Bokov and I. E. Mylnikova, (1960), Sov. Phys. Solid State 2, 2428.

Vittayakorn N., (2004), “The morphotropic phase boundary and dielectric properties of the $xPb(Zr_{1/2}Ti_{1/2})O_3$-$(1-x)Pb(Ni_{1/3}Nb_{2/3})O_3$ perovskite solid solution” Journal of Applied Physics.

Web 1, (2017) http://www.americanpiezo.com/piezo_theory/piezoelectric_constants.html (Access Date: 09.12.2017).

Web 2, (2018) http://sunnytec-piezo.com/en/productview.asp?id=170 (Access Date: 19.01.2018).

Wersing W., (1986), in Proceedings of 6th IEEE International Symposium on Application of Ferroelectrics, 212, 8–11.

BIOGRAPHY

Mehmet Gürkan Özyazıcı was born in Gaziantep in 1990. He lived in Gaziantep with his family until he finished his high school education. In 2009, he moved to İzmit, Kocaeli to study Metallurgical and Materials Engineering at Kocaeli University and graduated from his bachelor study in July 2014. He was accepted to Materials Science and Engineering department at Natural and Applied Sciences Institute at Gebze Technical University as a M.Sc. student in the next semester. In the end of fall semester of 2017-2018, he was completed his master study successfully.